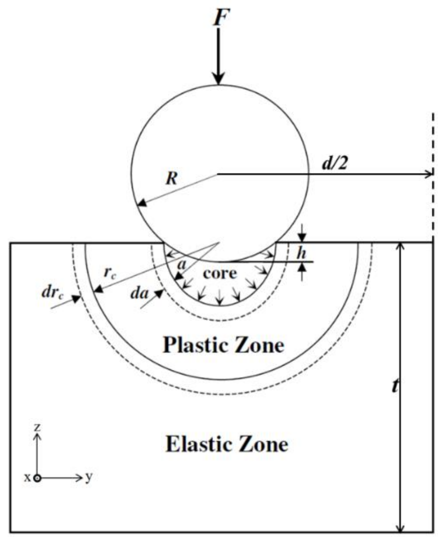

Fig. 1. Schematic showing of the expanding cavity model [46] indentation specimens. Here, R is the indenter radius, d is the width of specimens, t is the thickness, and a and r_c are the inner and outside radius of the plastic zone, respectively.

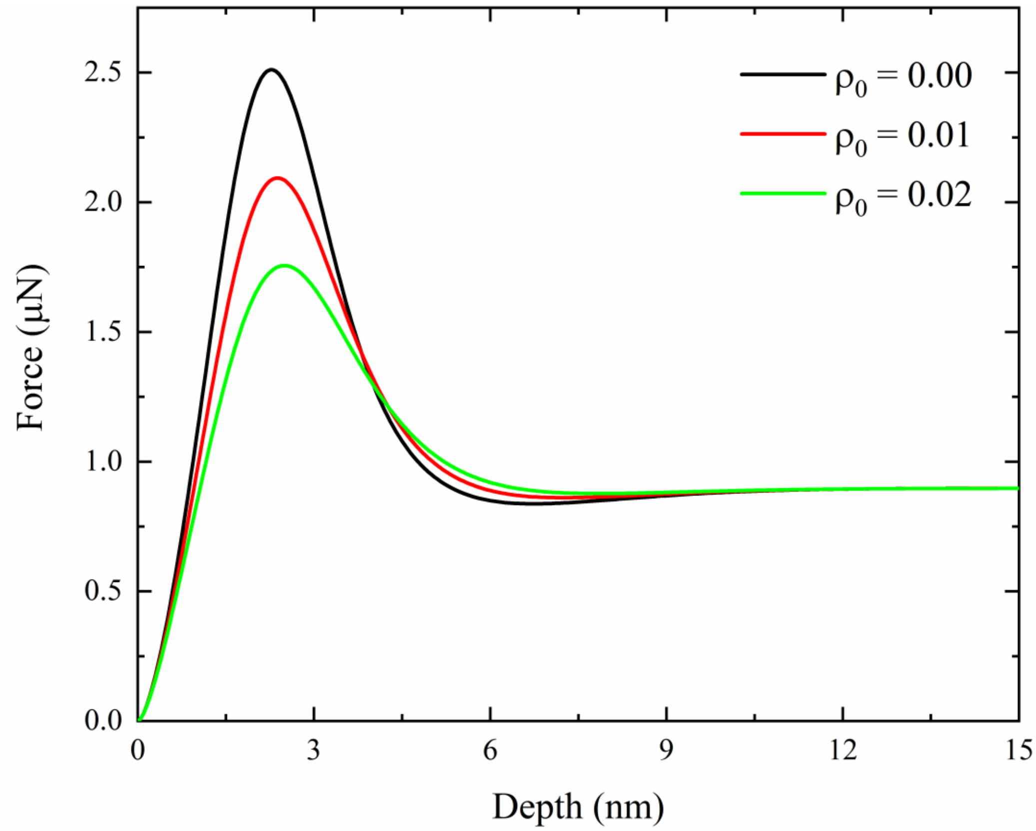

Fig. 2. The predicted force-depth curves with different initial dislocation densities in the unit of nm^{-2}.

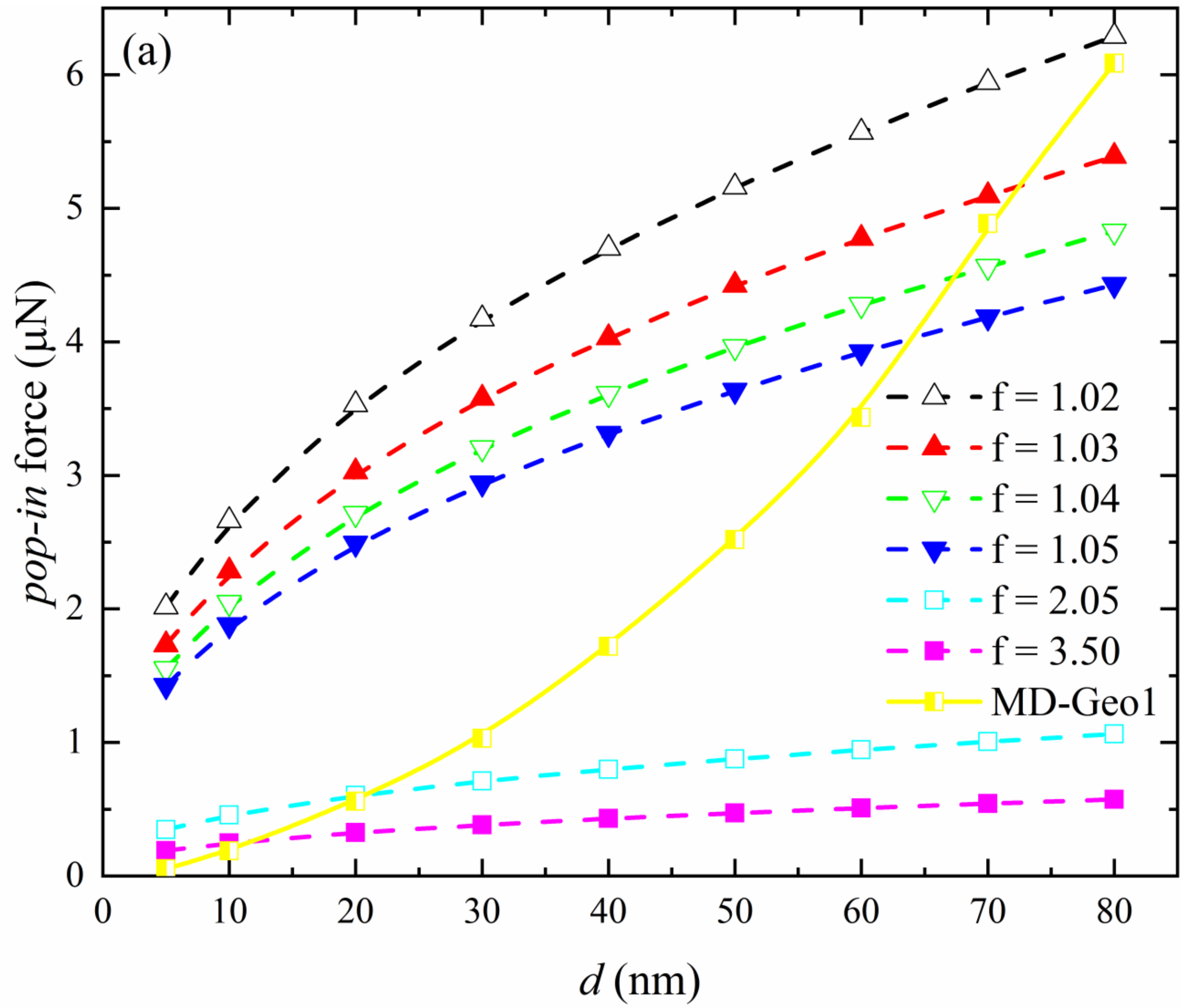

(a)
pop-in force (μN)
d (nm)
f = 1.02
f = 1.03
f = 1.04
f = 1.05
f = 2.05
f = 3.50
MD-Geo1
0
1
2
3
4
5
6
0
10
20
30
40
50
60
70
80

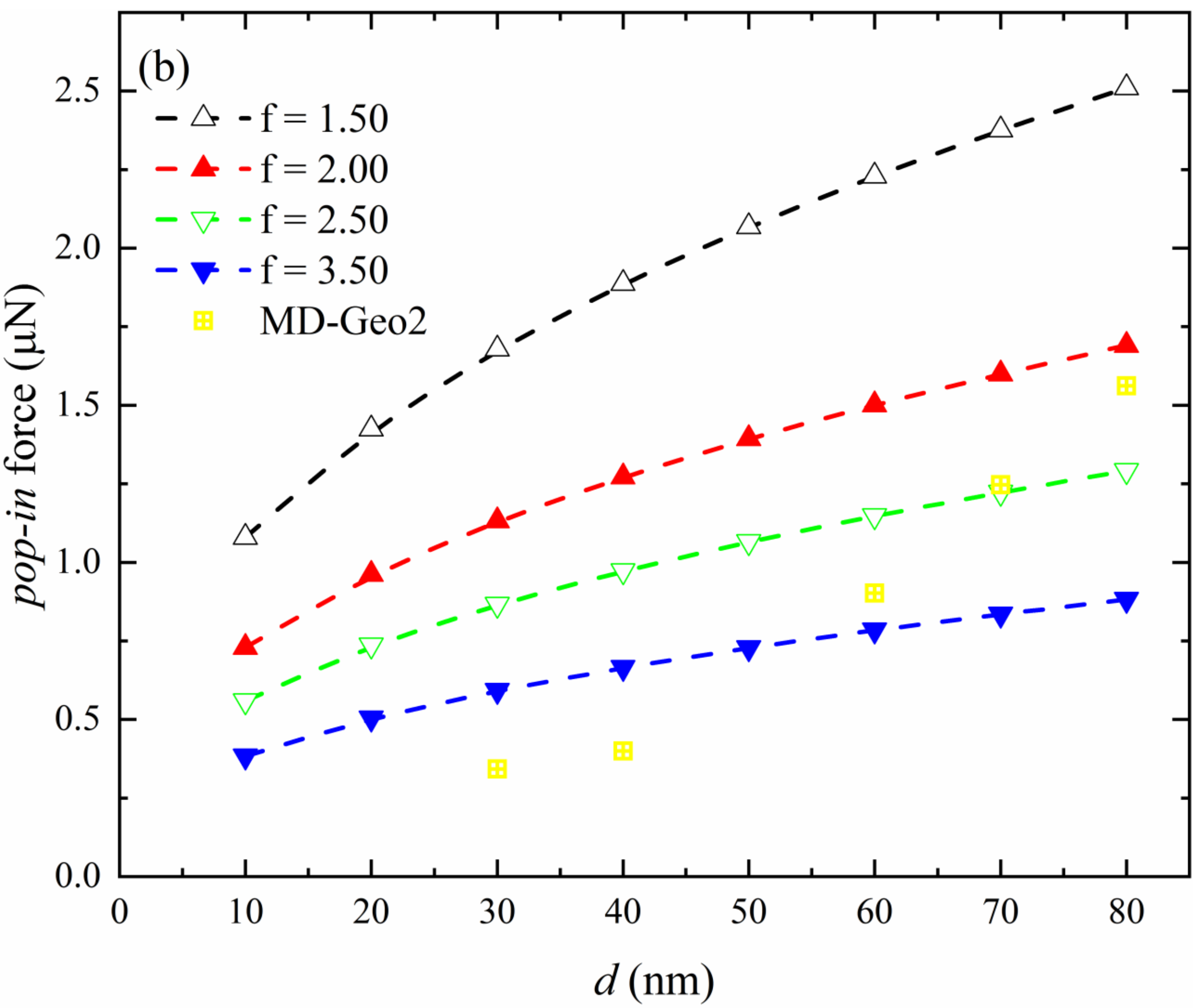

(b)
f = 1.50
f = 2.00
f = 2.50
f = 3.50
MD-Geo2
pop-in force (μN)
d (nm)
0.0
0.5
1.0
1.5
2.0
2.5
0
10
20
30
40
50
60
70
80

1

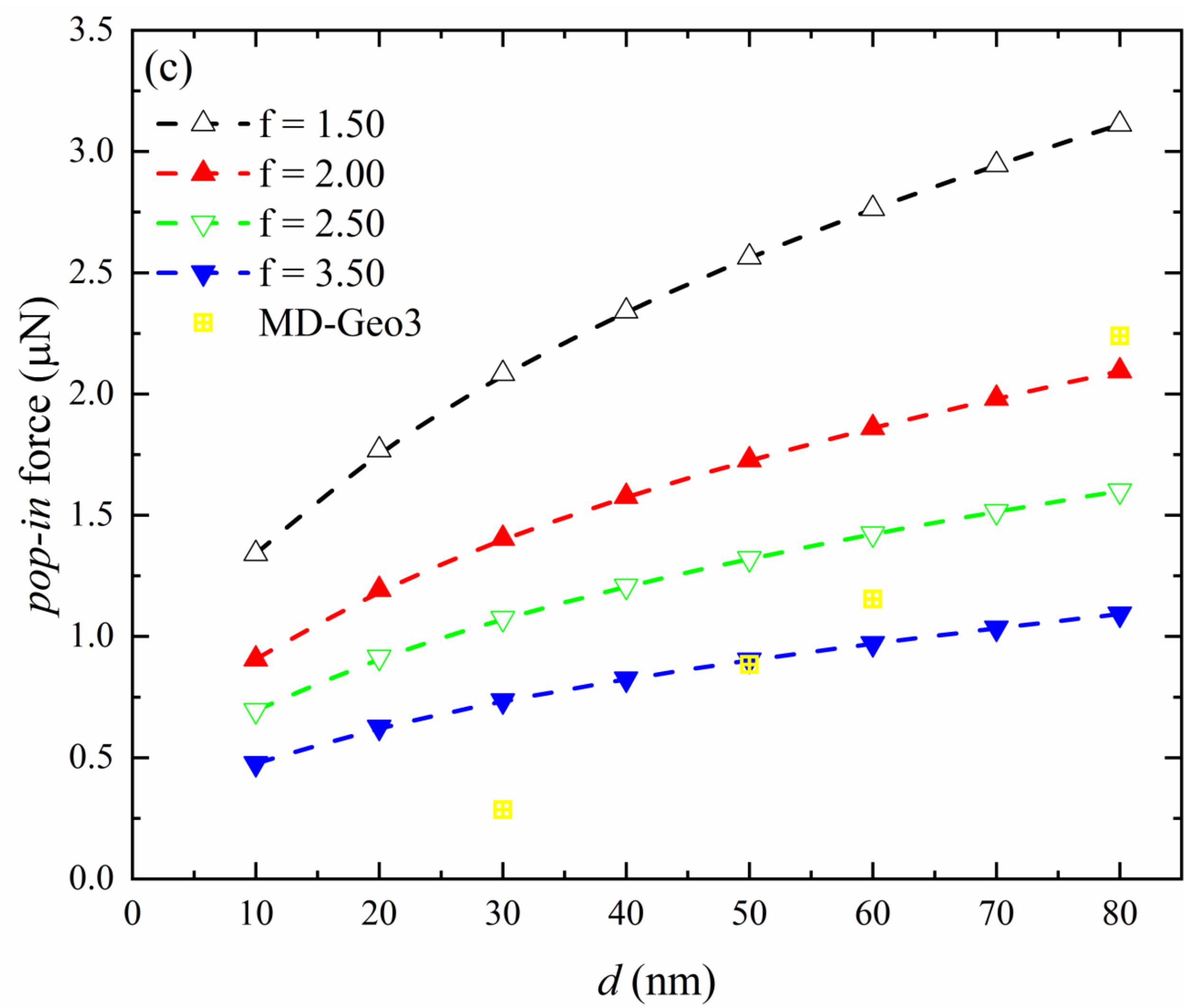
(c)
f = 1.50
f = 2.00
f = 2.50
f = 3.50
MD-Geo3
pop-in force (μN)
d (nm)
0.0
0.5
1.0
1.5
2.0
2.5
3.0
3.5
0
10
20
30
40
50
60
70
80

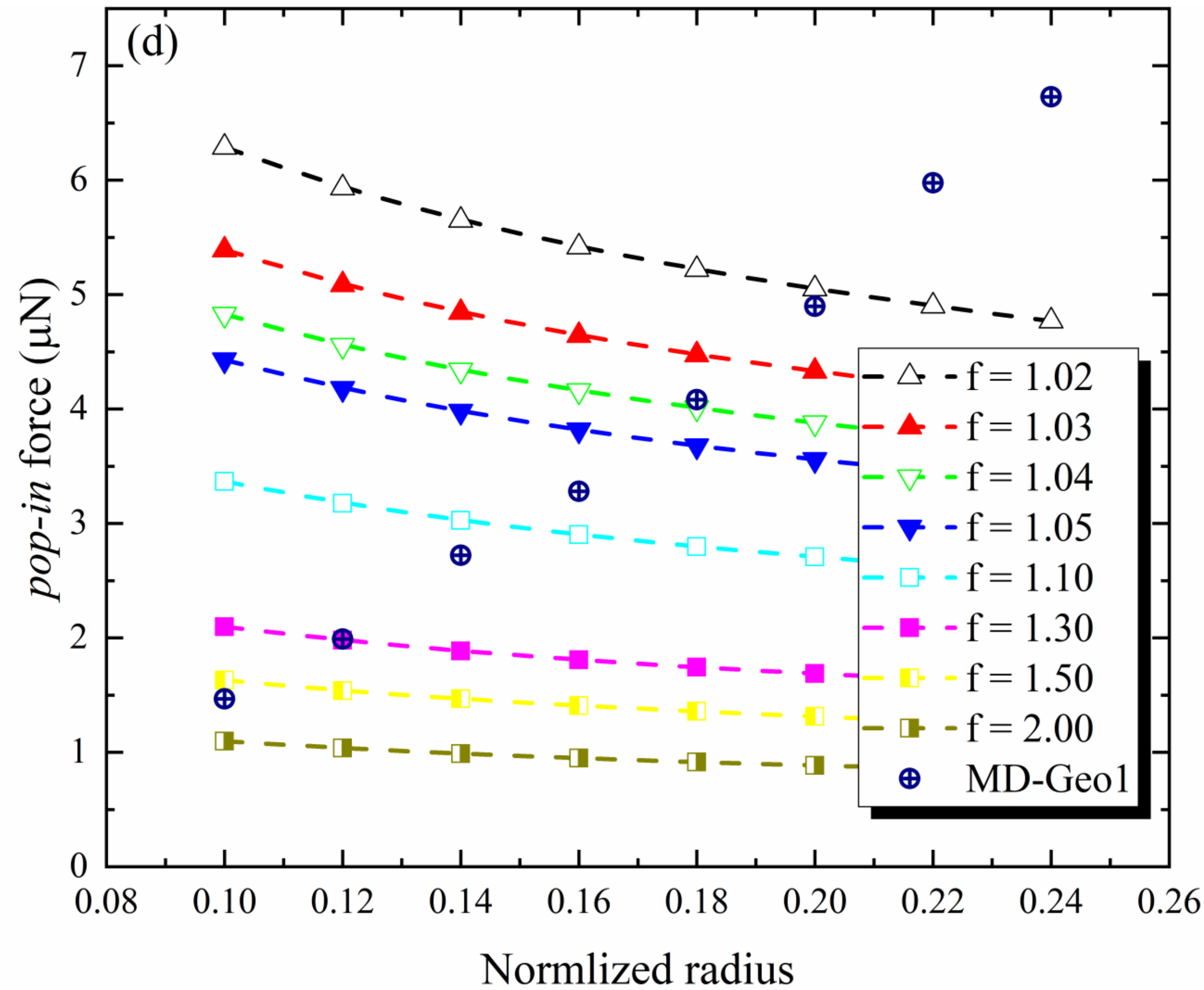

(d)
pop-in force (μN)
Normlized radius
0
1
2
3
4
5
6
7
0.08
0.10
0.12
0.14
0.16
0.18
0.20
0.22
0.24
0.26
f = 1.02
f = 1.03
f = 1.04
f = 1.05
f = 1.10
f = 1.30
f = 1.50
f = 2.00
MD-Geo1

1

1 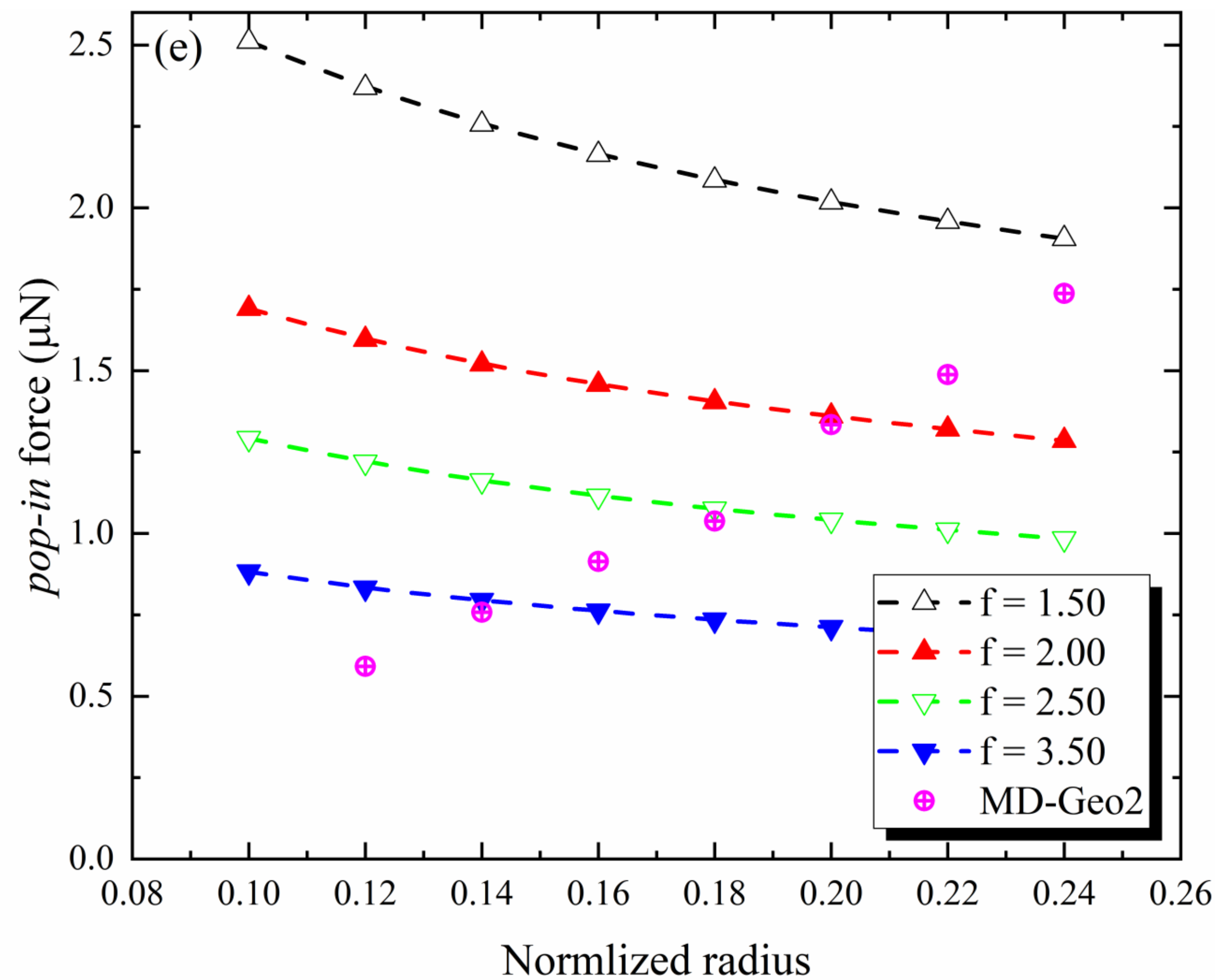

(e)
pop-in force (μN)
Normlized radius
2.5
2.0
1.5
1.0
0.5
0.0
0.08
0.10
0.12
0.14
0.16
0.18
0.20
0.22
0.24
0.26
f = 1.50
f = 2.00
f = 2.50
f = 3.50
MD-Geo2

1 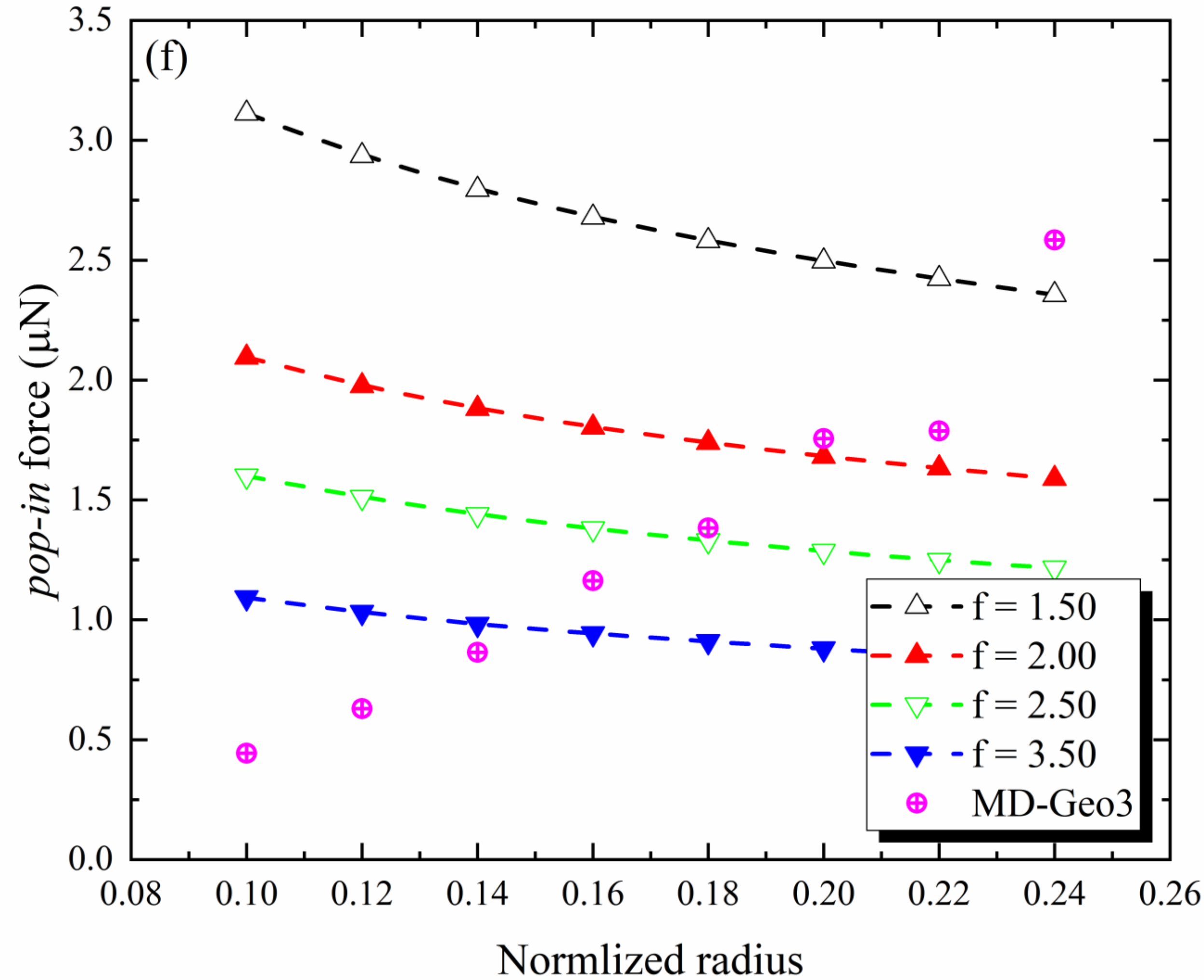

(f)
pop-in force (μN)
Normlized radius
f = 1.50
f = 2.00
f = 2.50
f = 3.50
MD-Geo3
3.5
3.0
2.5
2.0
1.5
1.0
0.5
0.0
0.08
0.10
0.12
0.14
0.16
0.18
0.20
0.22
0.24
0.26

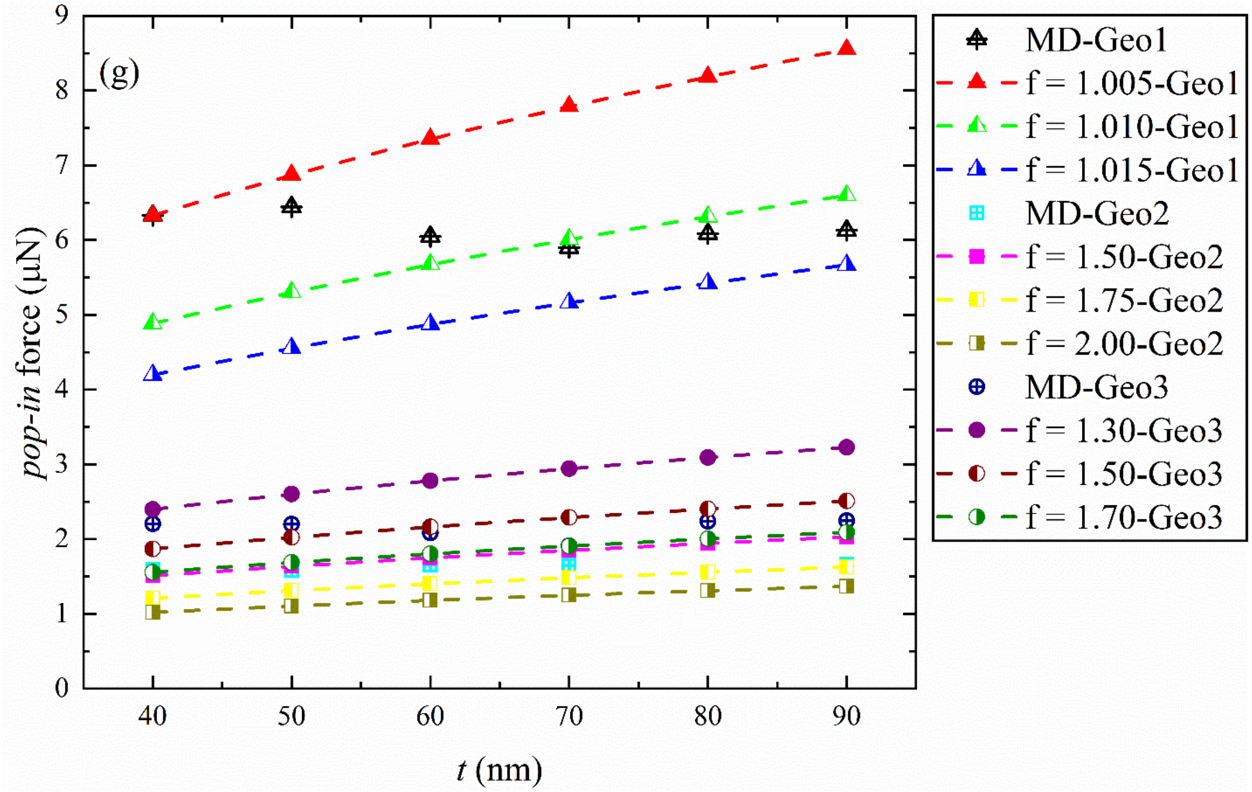
(g)
pop-in force (μN)
t (nm)
0
1
2
3
4
5
6
7
8
9
40
50
60
70
80
90
MD-Geo1
f = 1.005-Geo1
f = 1.010-Geo1
f = 1.015-Geo1
MD-Geo2
f = 1.50-Geo2
f = 1.75-Geo2
f = 2.00-Geo2
MD-Geo3
f = 1.30-Geo3
f = 1.50-Geo3
f = 1.70-Geo3

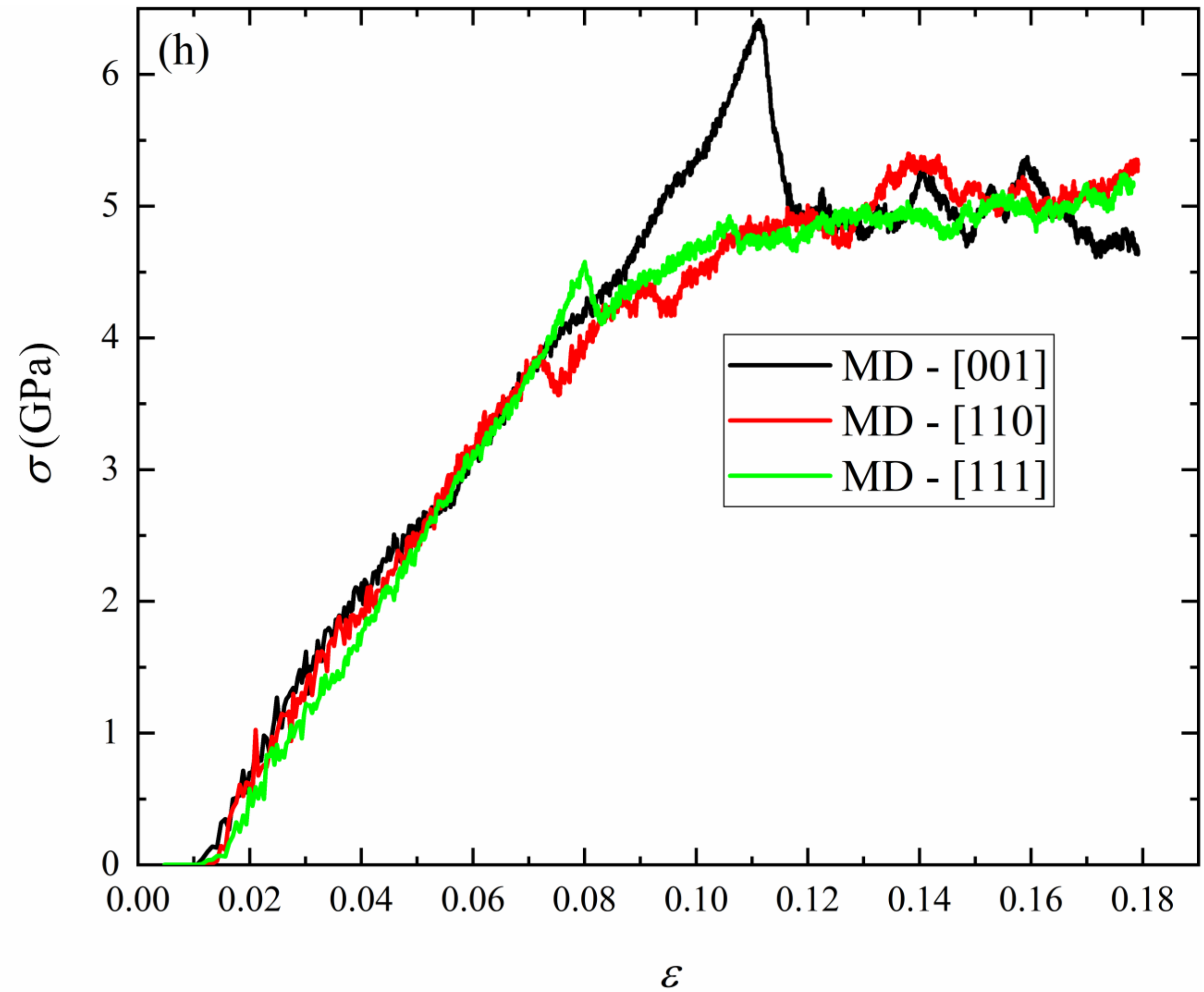

Fig. 3. Effect of geometry size on mechanical response of the Fe specimens under nanoindentation loading. (a) width d; (b) normalized radius R/d; (c) thickness t; (d) derived stress-strain curves under uniaxial compression for the specimens with $d, t =$ 80 nm, $R/d = 0.225$, and $v_i = 0.5$ Å/ps.

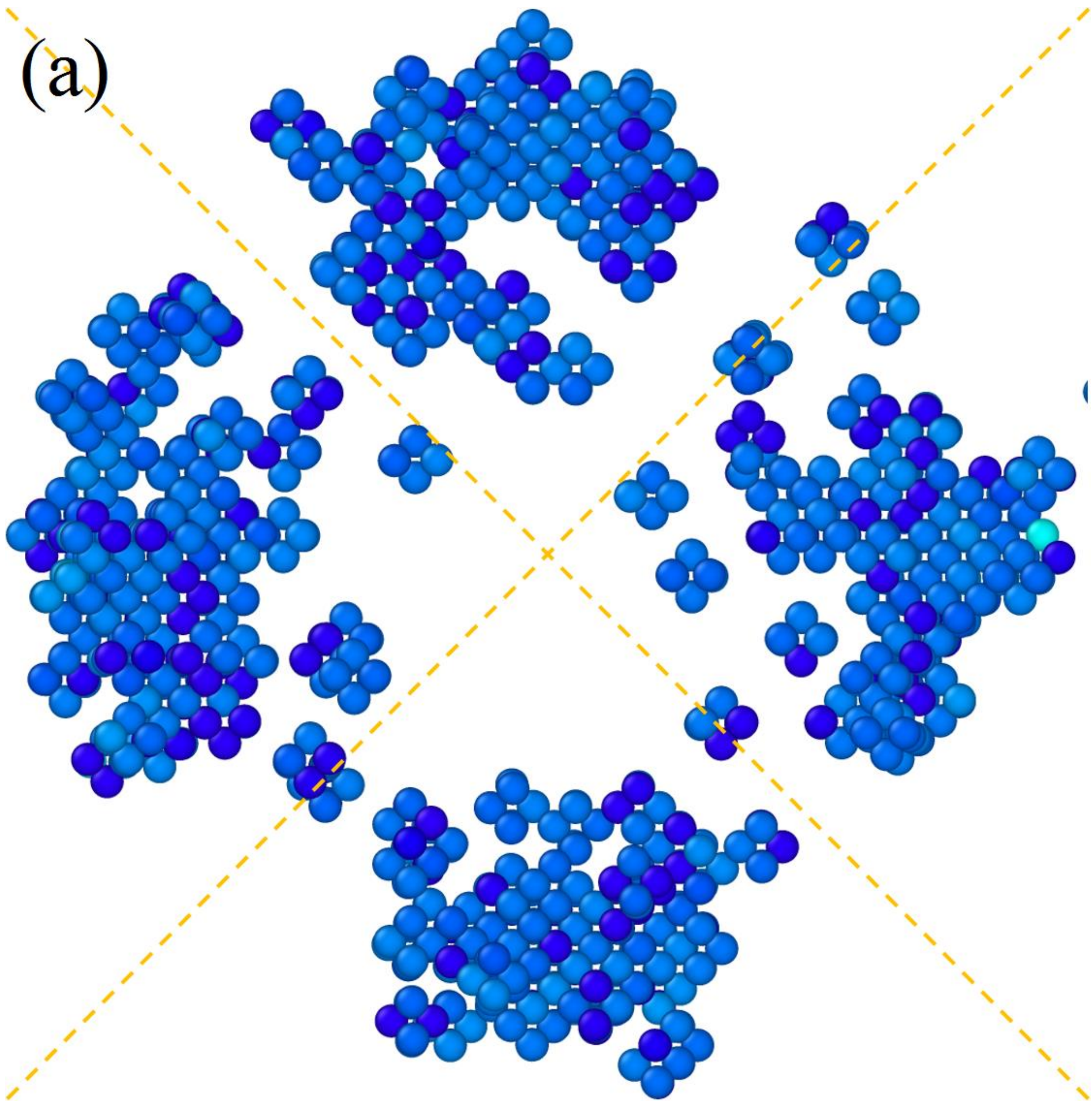
(a)

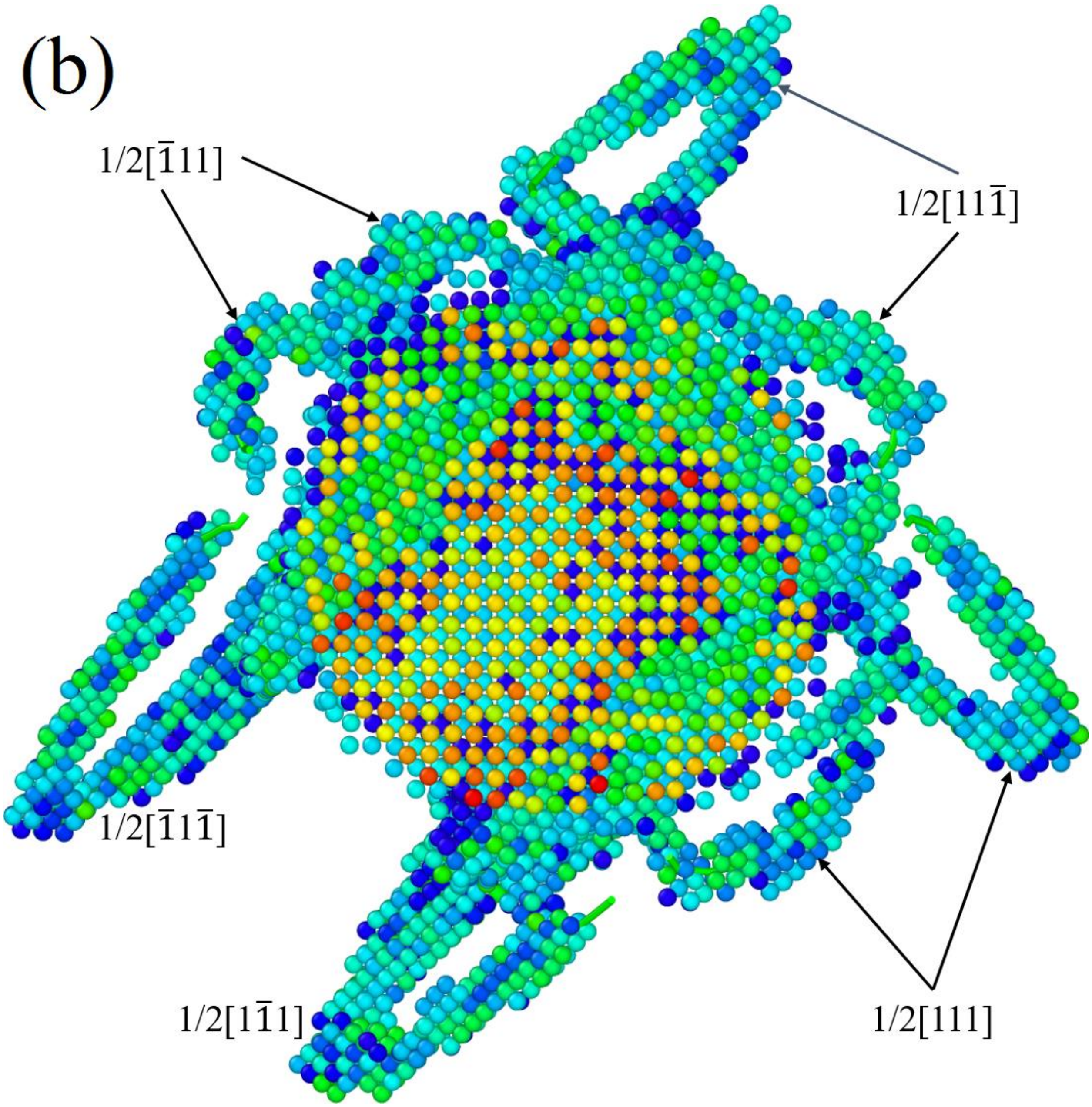
(b)
$1/2[\bar{1}11]$
$1/2[11\bar{1}]$
$1/2[\bar{1}1\bar{1}]$
$1/2[1\bar{1}1]$
$1/2[111]$

(c)

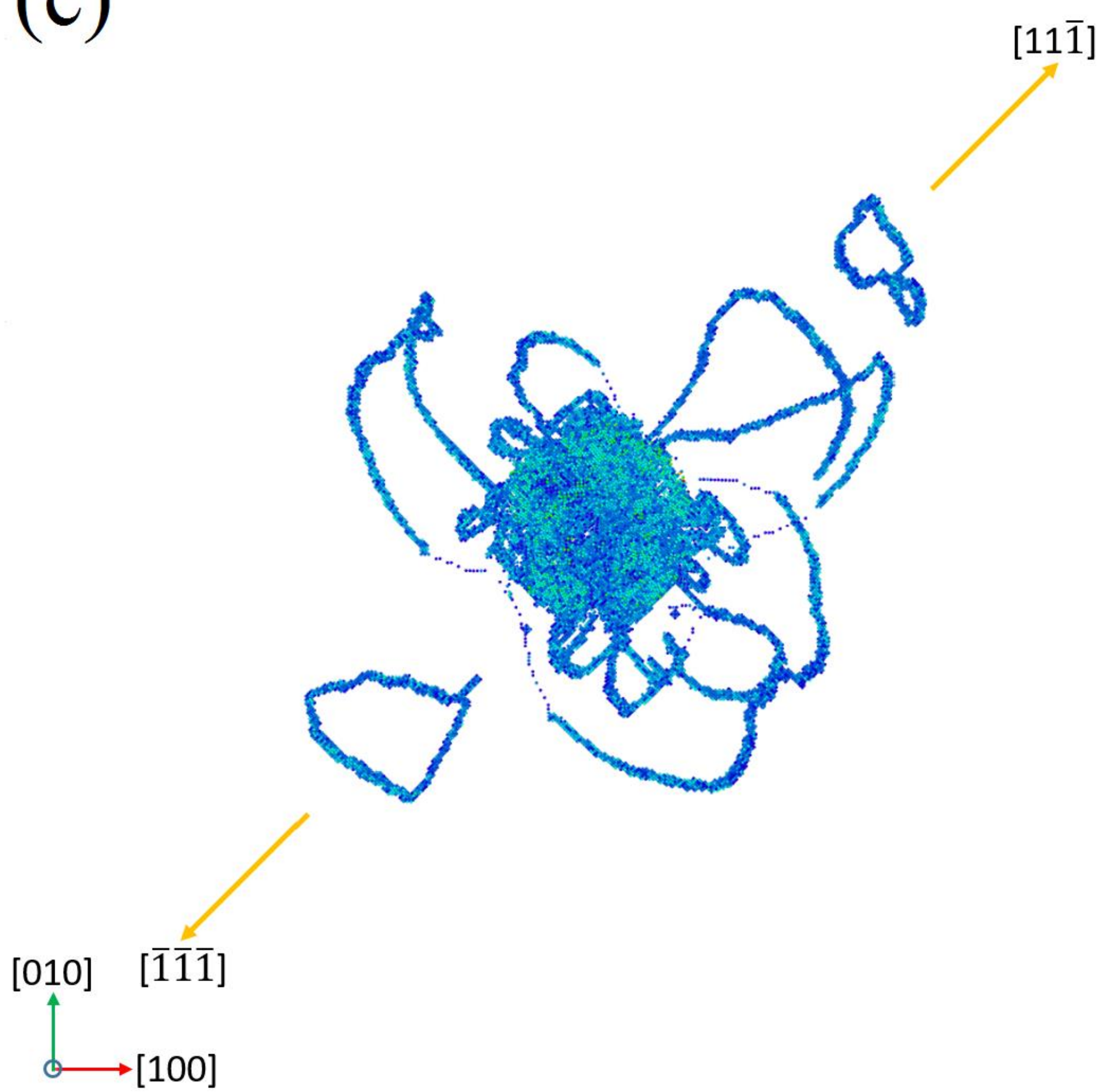

1

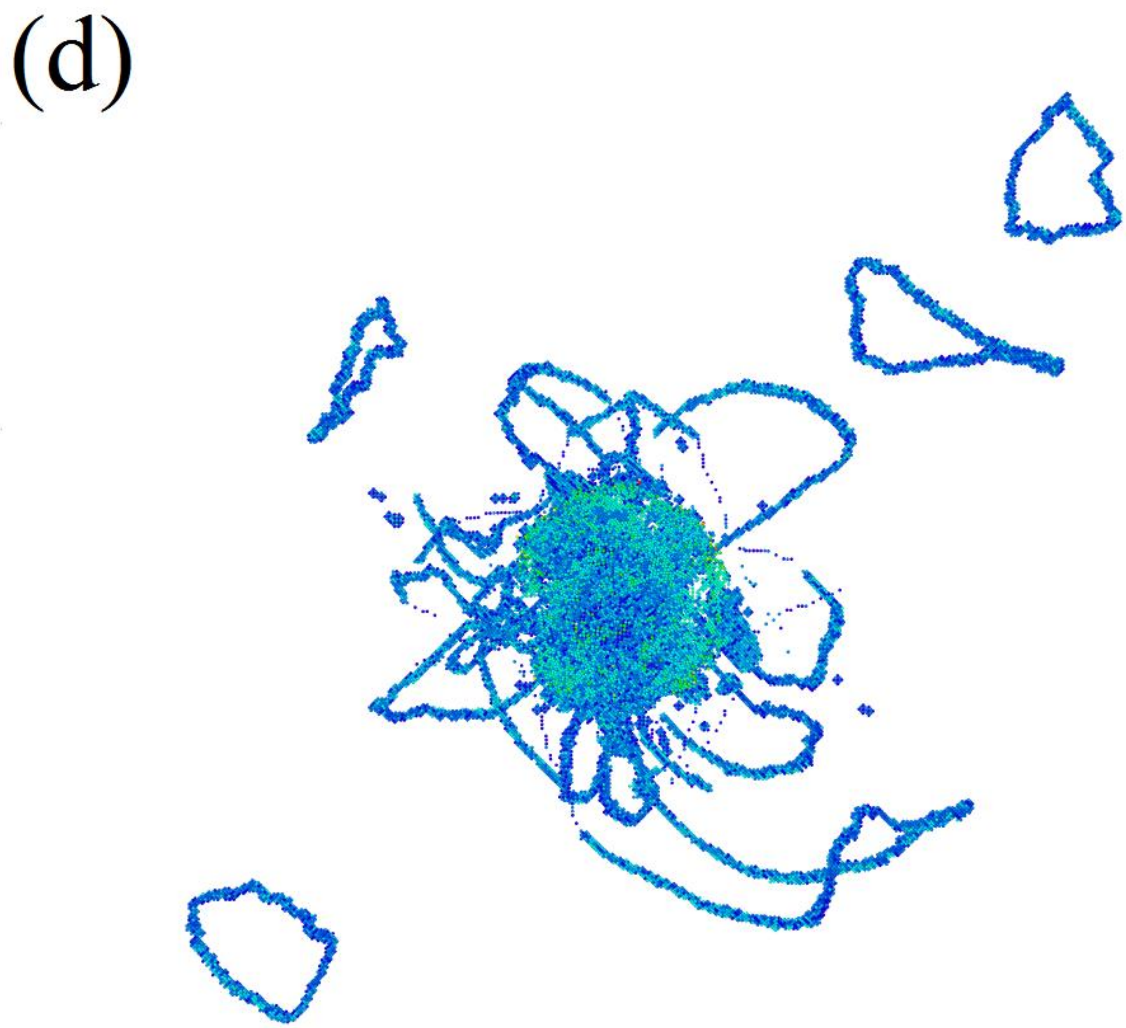

Fig. 4. Snapshots for the nanoindentation of Geo1 specimens. (a) Top view at h = 17 Å, FOS clusters are formed under the indenter, and the cross-section of the indenter and the top-surface is shown by the orange circle; (b) h = 18 Å, $1/2\langle 111\rangle$ shear loops are emitted; (c) h = 40 Å, prismatic loops are generated along $[11\bar{1}]$ and $[\bar{1}\bar{1}\bar{1}]$ directions; (d) h = 50 Å, a new prismatic loop is generated along $[\bar{1}1\bar{1}]$. The atoms are colored according to CNA values, all the normal bcc atoms have been deleted.

1 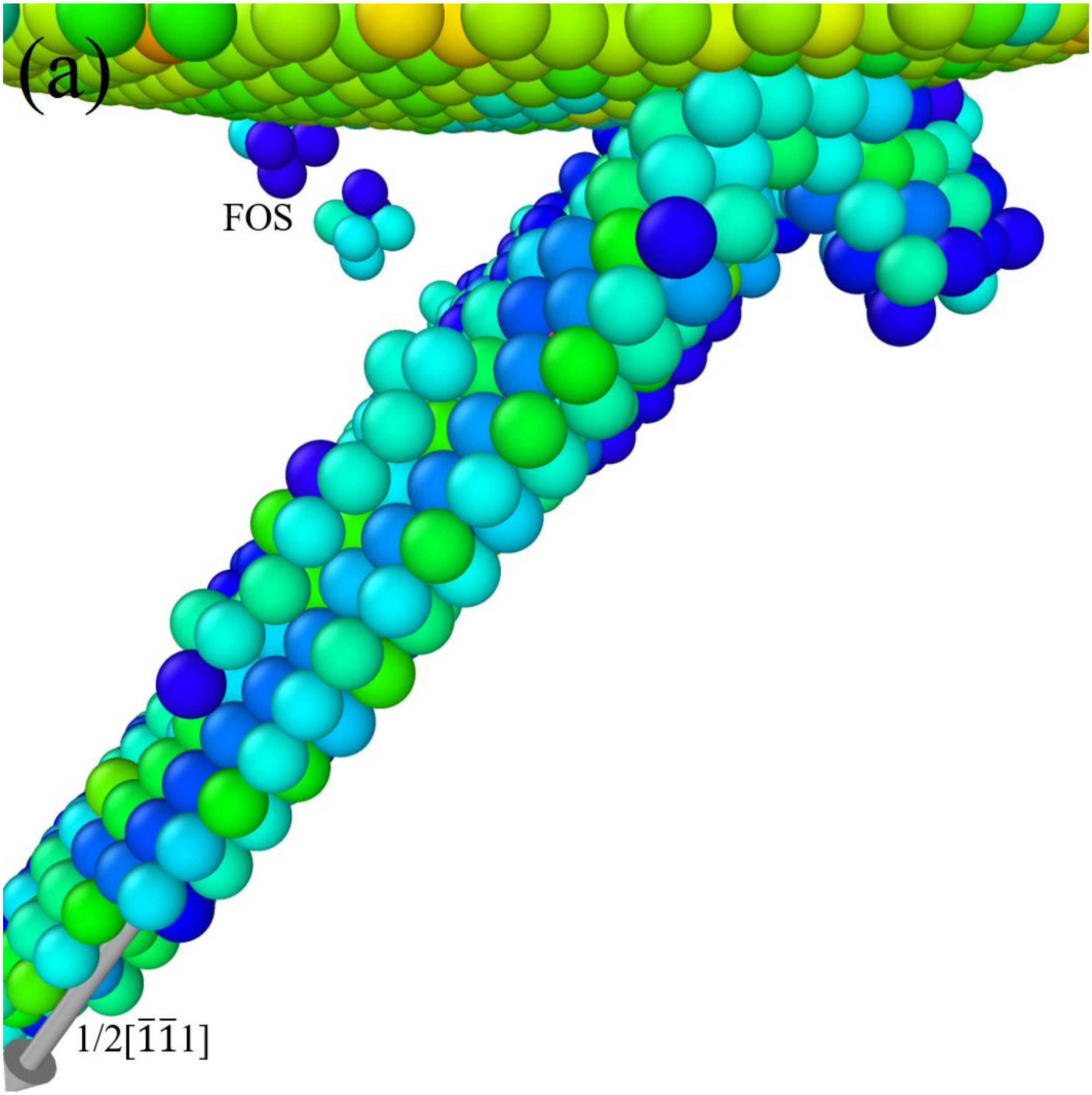

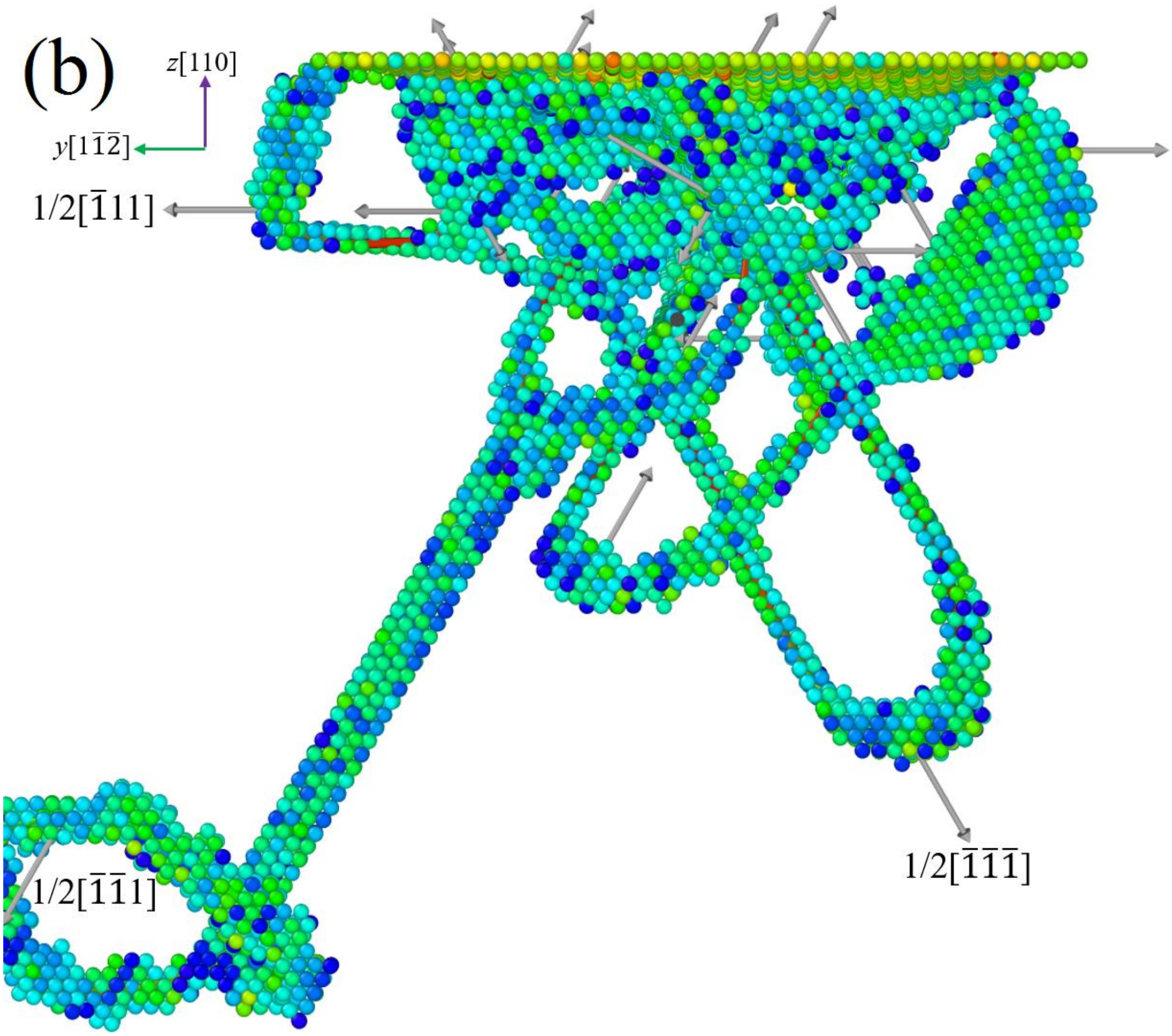

1

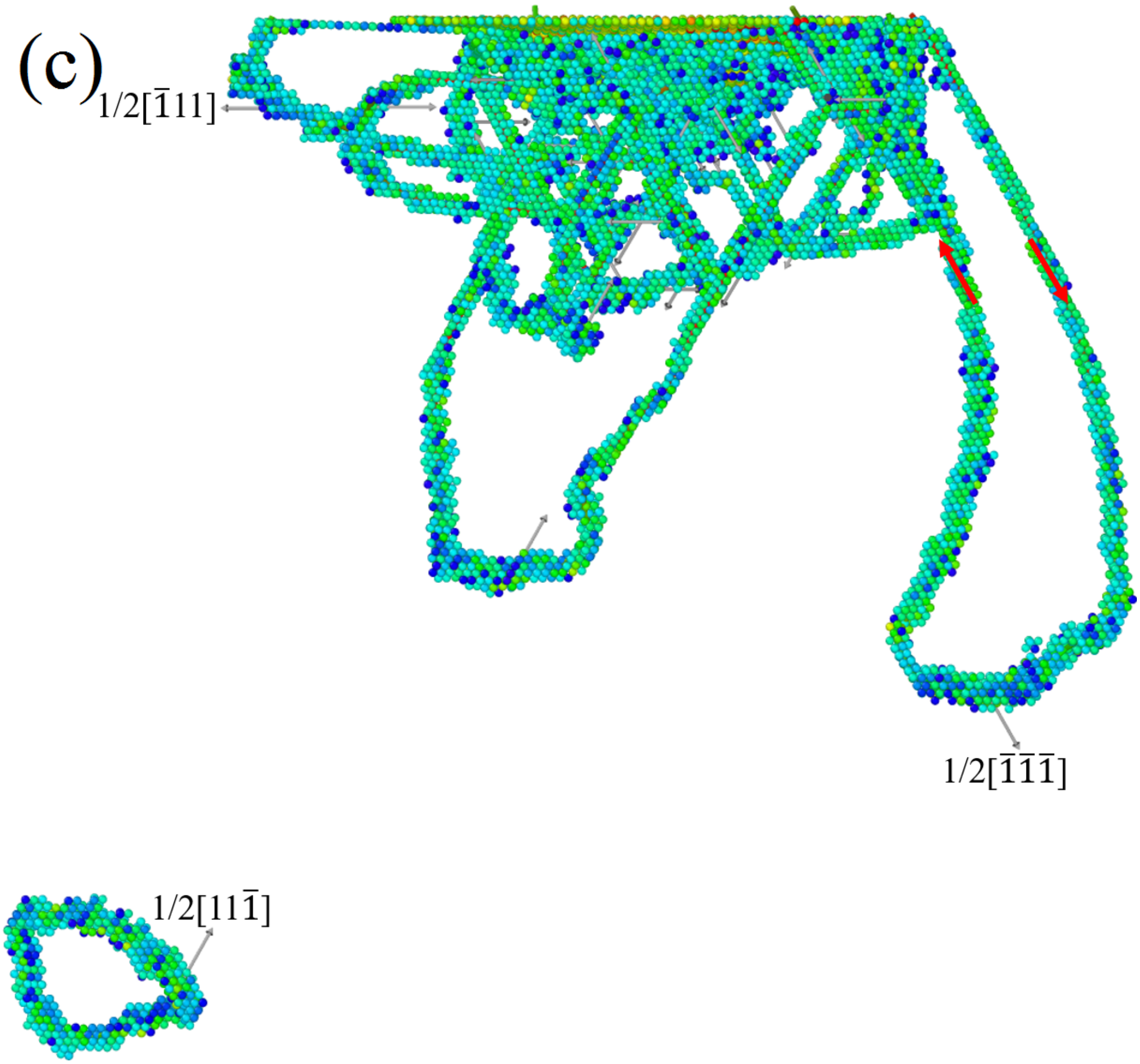
(c)
$1/2[\bar{1}11]$
$1/2[\bar{1}\bar{1}\bar{1}]$
$1/2[11\bar{1}]$

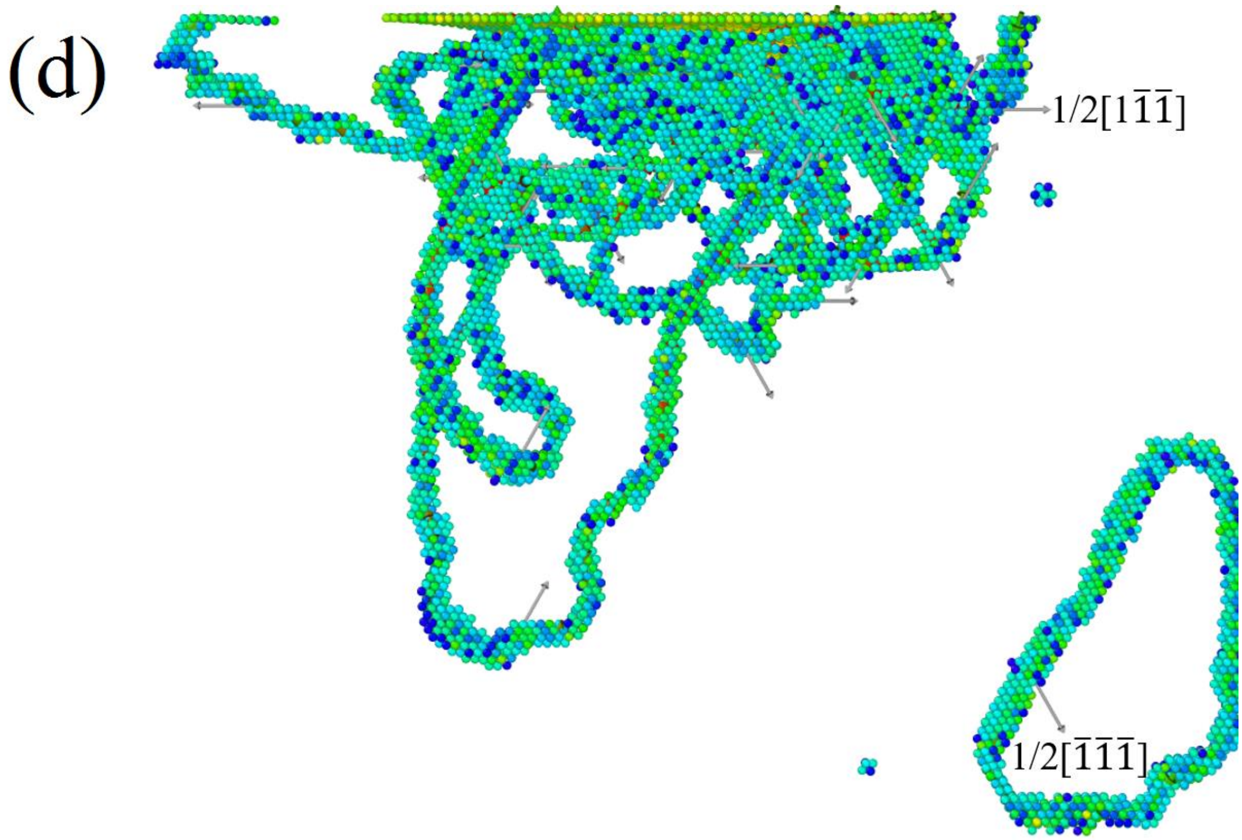

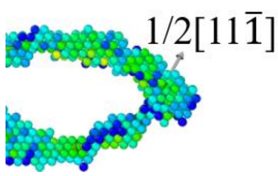

Fig. 5. Snapshots for the nanoindentation of Geo2 specimens. (a) h = 8 Å, all regular bcc atoms are deleted, and the indenter is shown by a red curve; (b) h = 16 Å, a prismatic loop is formed by 'lasso' action; (c) h = 24 Å, the 1/2[11$\bar{1}$] loop detached from the screw components, of which the line directions are marked by red arrows; (d) h = 26 Å, another 1/2[$\bar{1}\bar{1}\bar{1}$] loop is formed. The grey arrows represent Burgers vectors. The atoms are colored according to CNA values, and all the normal bcc atoms have been deleted.

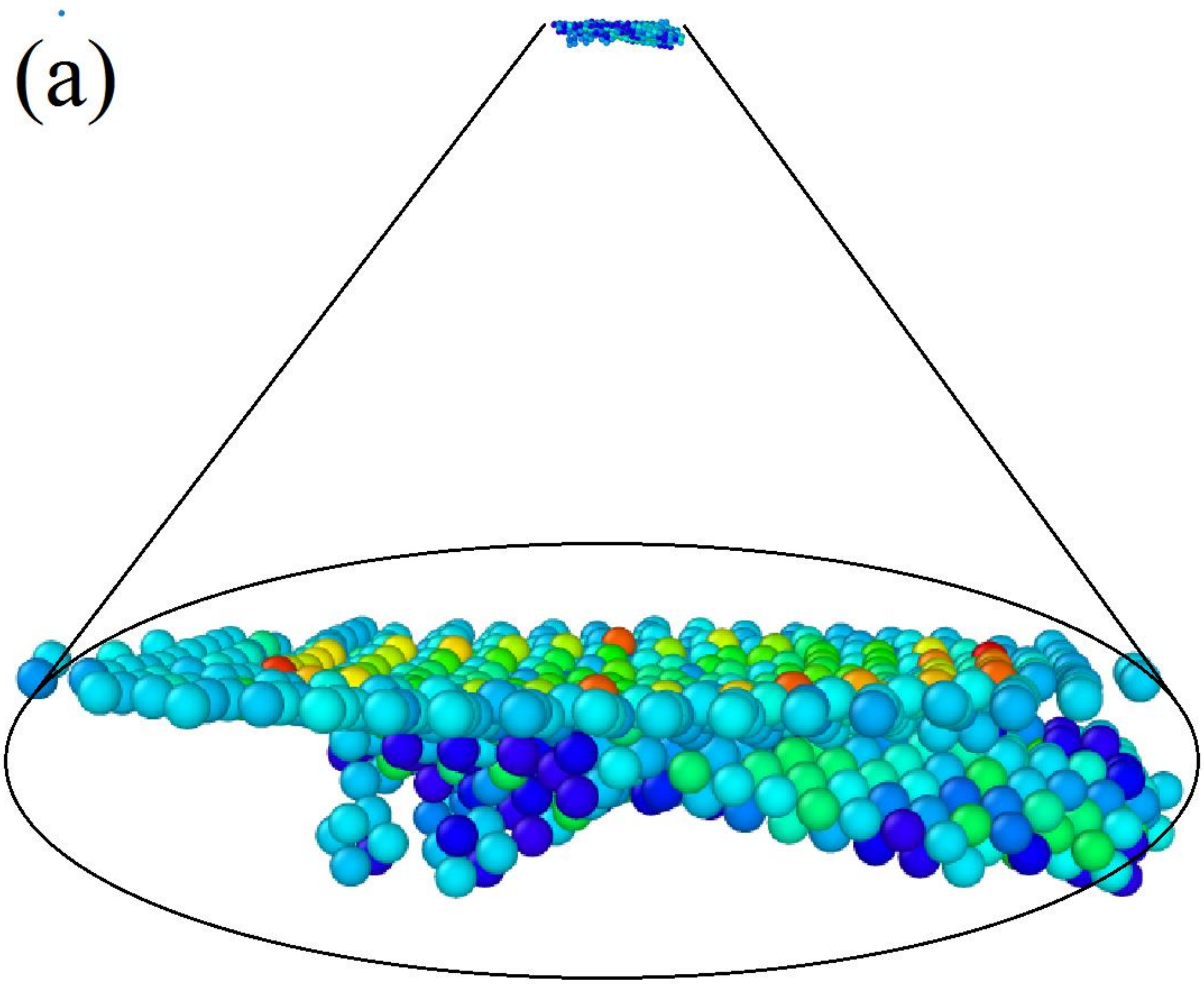
(a)

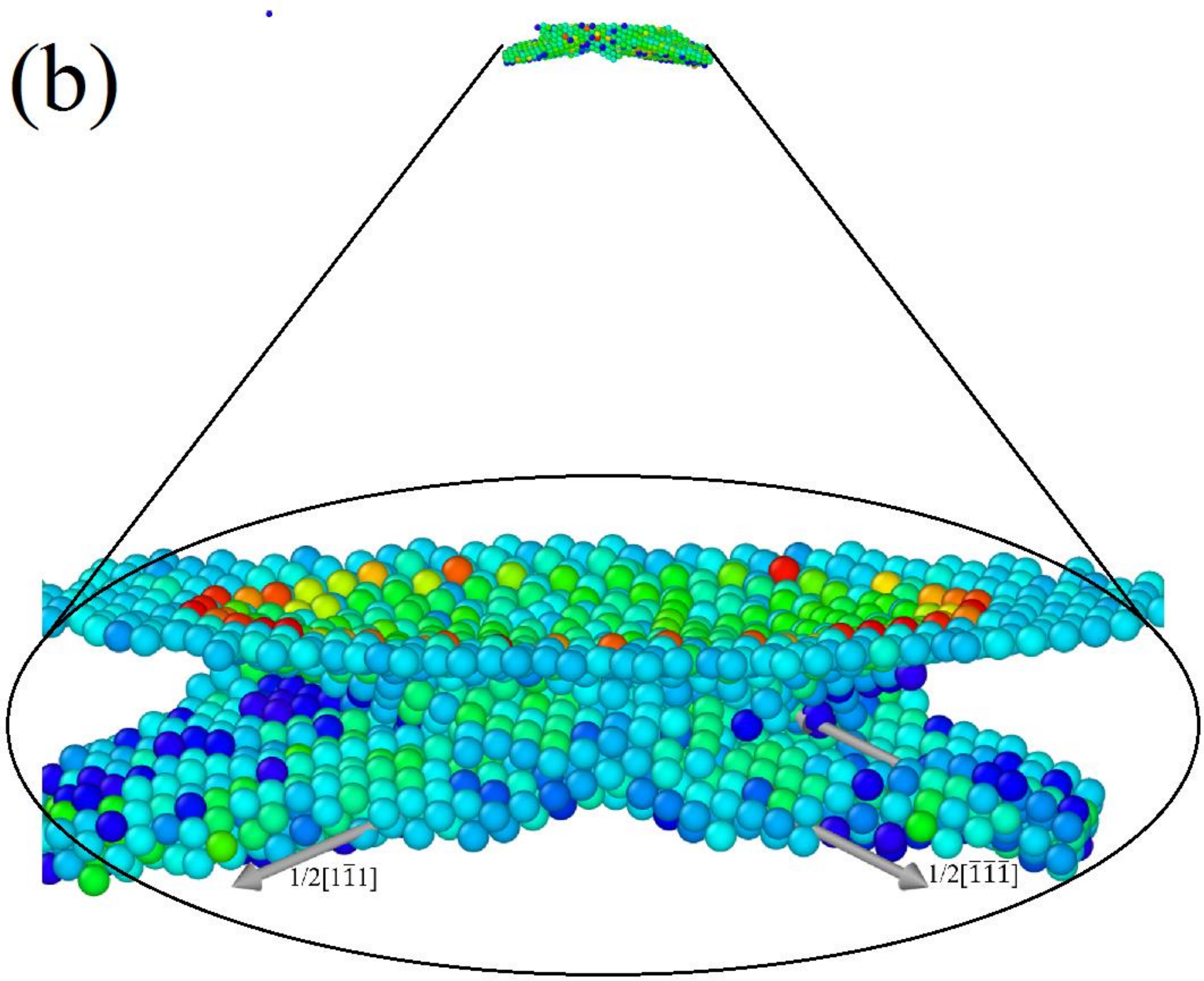
(b)
1/2[1$\bar{1}$1]
1/2[$\bar{1}\bar{1}\bar{1}$]

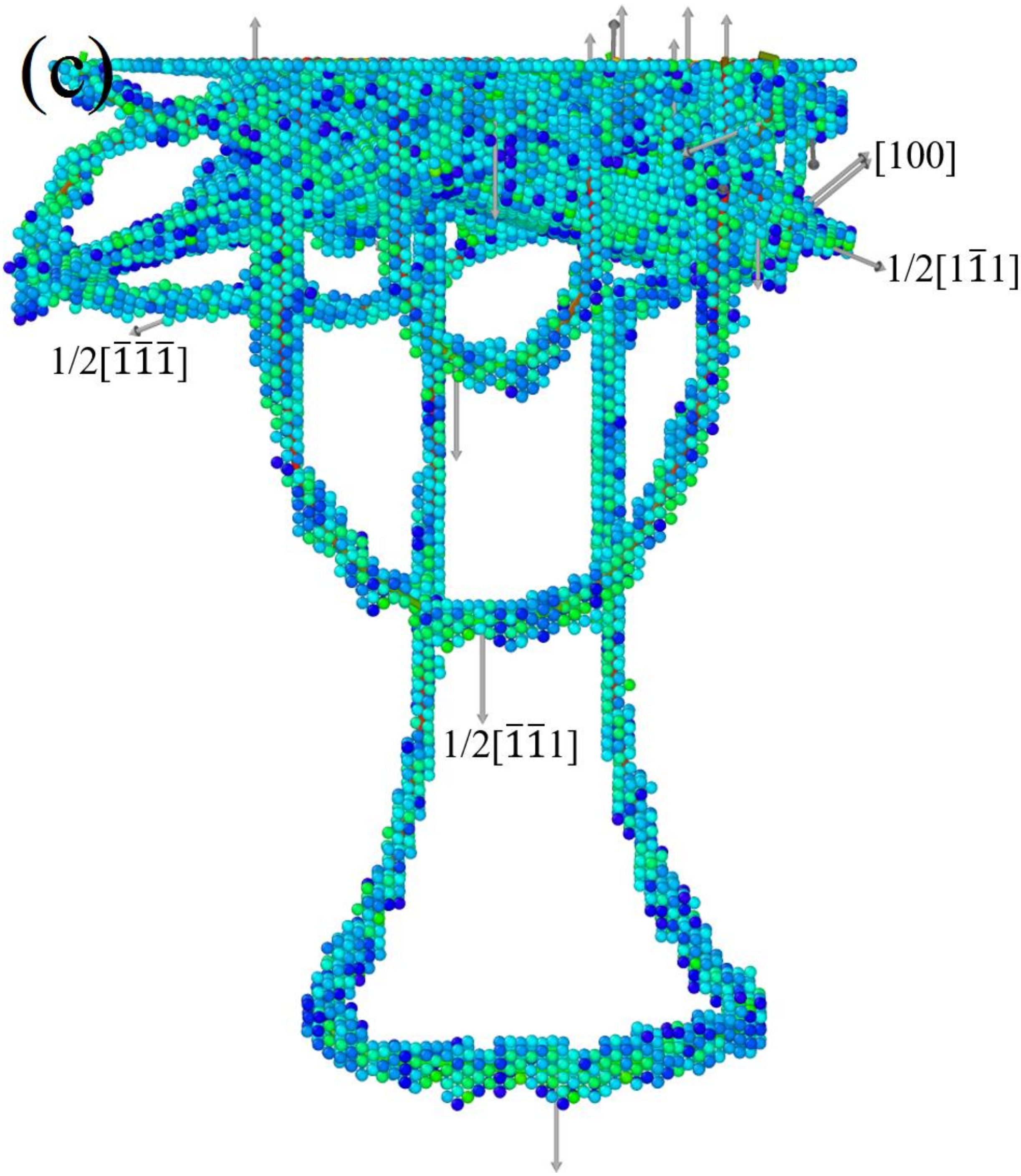
(c)
[100]
1/2[1$\bar{1}$1]
1/2[$\bar{1}\bar{1}\bar{1}$]
1/2[$\bar{1}\bar{1}$1]

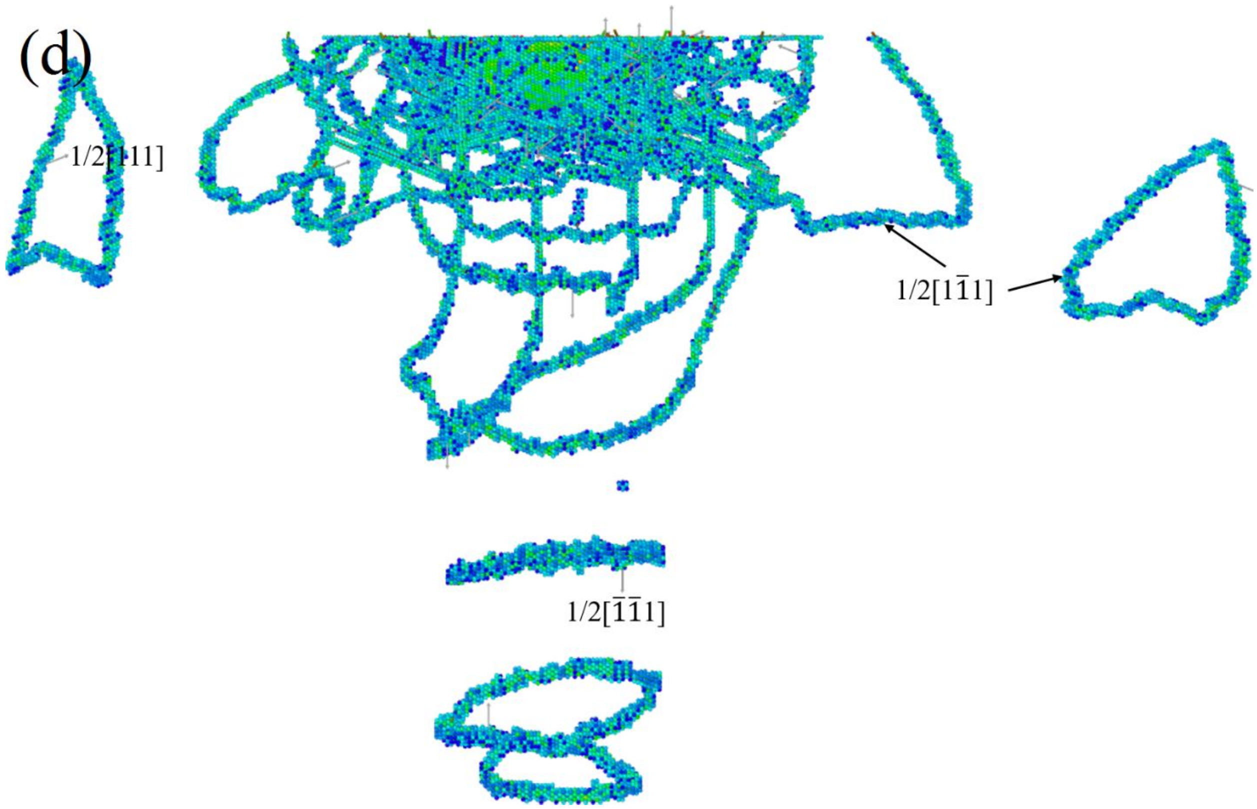

Fig. 6. Snapshots for the nanoindentation of Geo3 specimens. (a) h = 8 Å, no dislocation is detected; (b) h = 10 Å; (c) h = 20 Å; (d) h = 48 Å. The grey arrows represent Burgers vectors. The atoms are colored according to CNA values, and all the normal bcc atoms have been deleted.

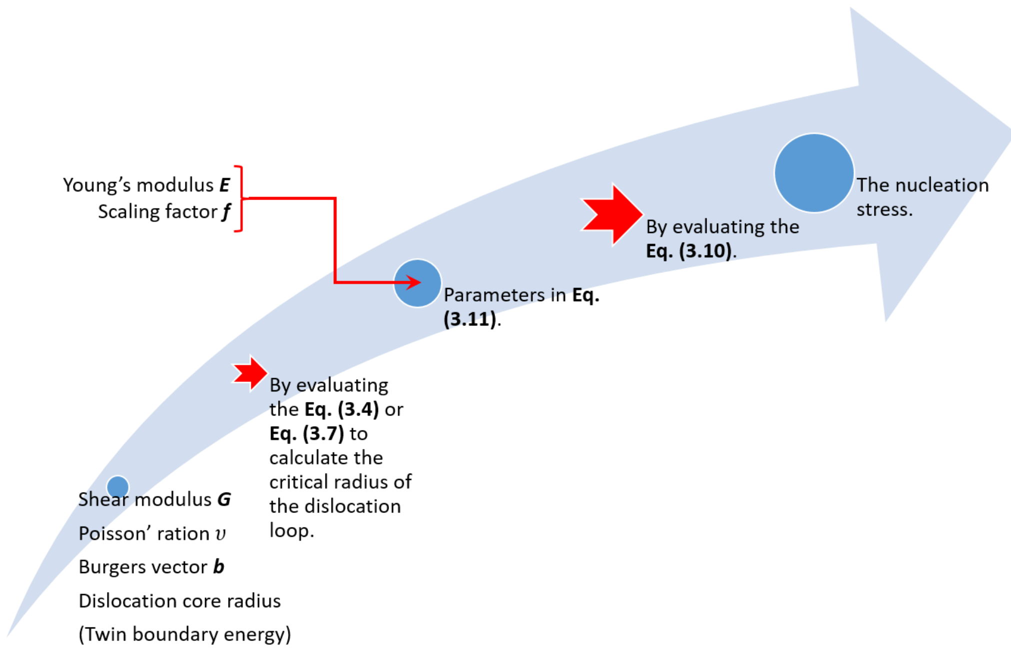

Fig. 7. The schematics of solving the nucleation stress under the framework of TST.

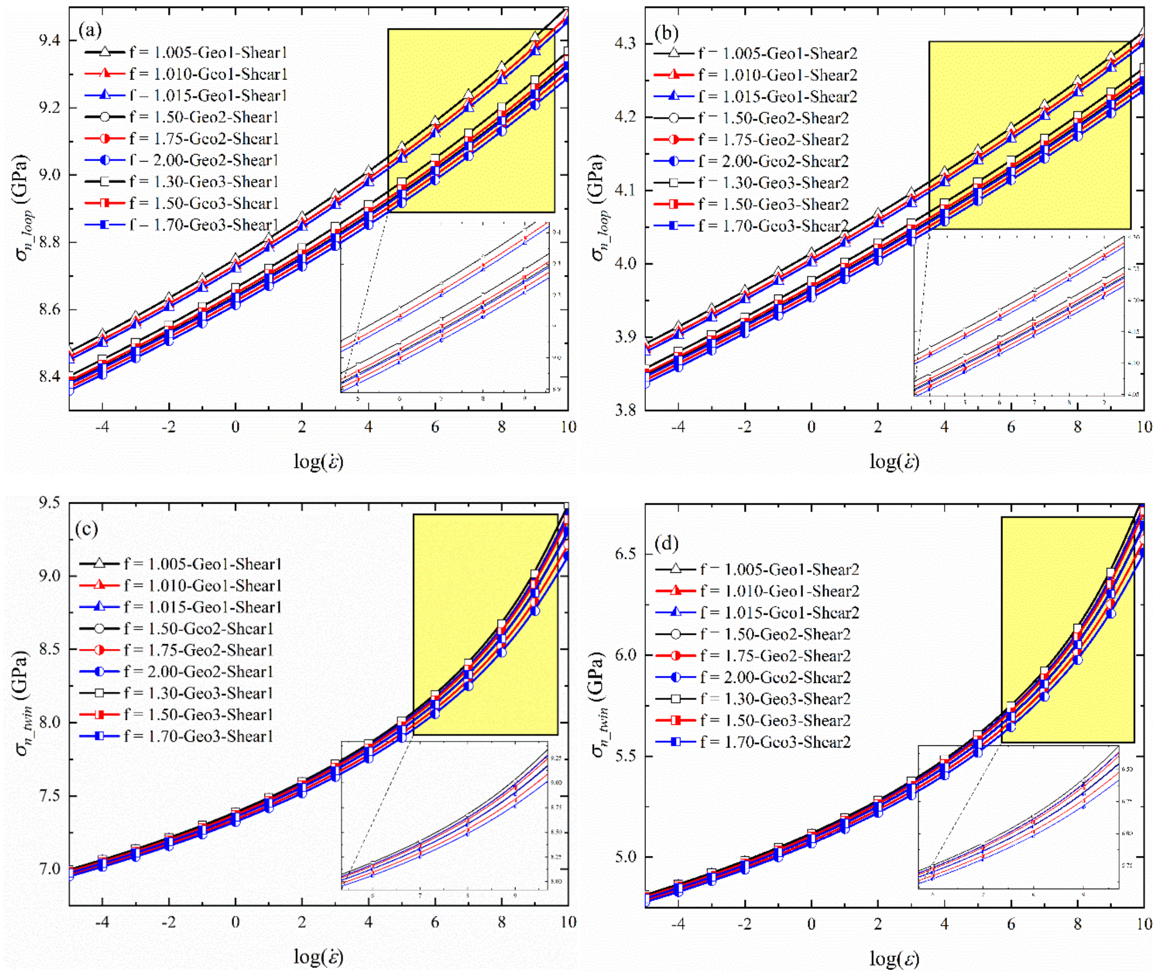

Fig. 8. The nucleation stress as a function of strain rate, derived from the classical nucleation theory **Eq. (3.8)**.

1

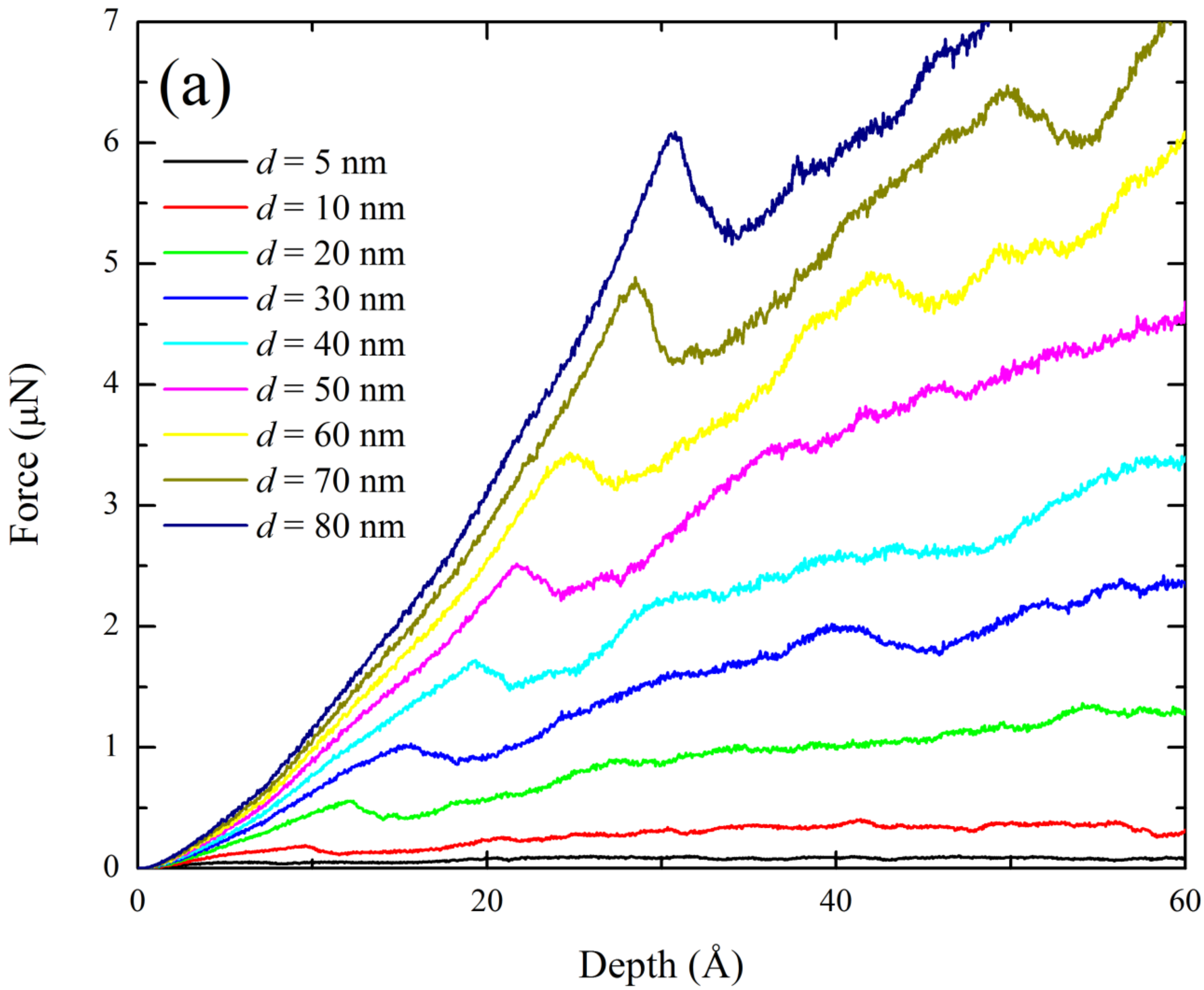
(a)
d = 5 nm
d = 10 nm
d = 20 nm
d = 30 nm
d = 40 nm
d = 50 nm
d = 60 nm
d = 70 nm
d = 80 nm
Force (μN)
Depth (Å)
0
1
2
3
4
5
6
7
0
20
40
60

1 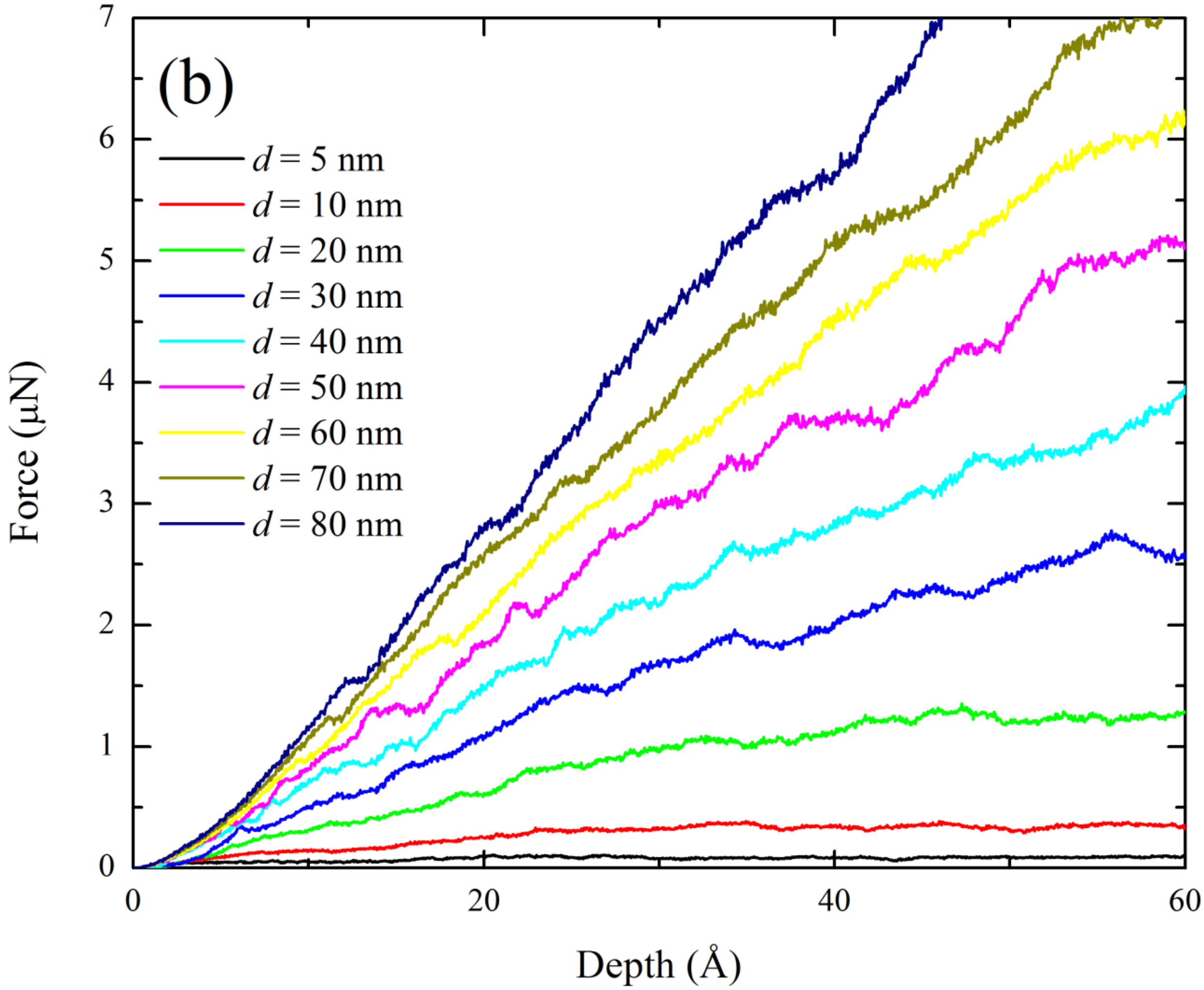

(b)
d = 5 nm
d = 10 nm
d = 20 nm
d = 30 nm
d = 40 nm
d = 50 nm
d = 60 nm
d = 70 nm
d = 80 nm
Force (μN)
Depth (Å)
0
1
2
3
4
5
6
7
0
20
40
60

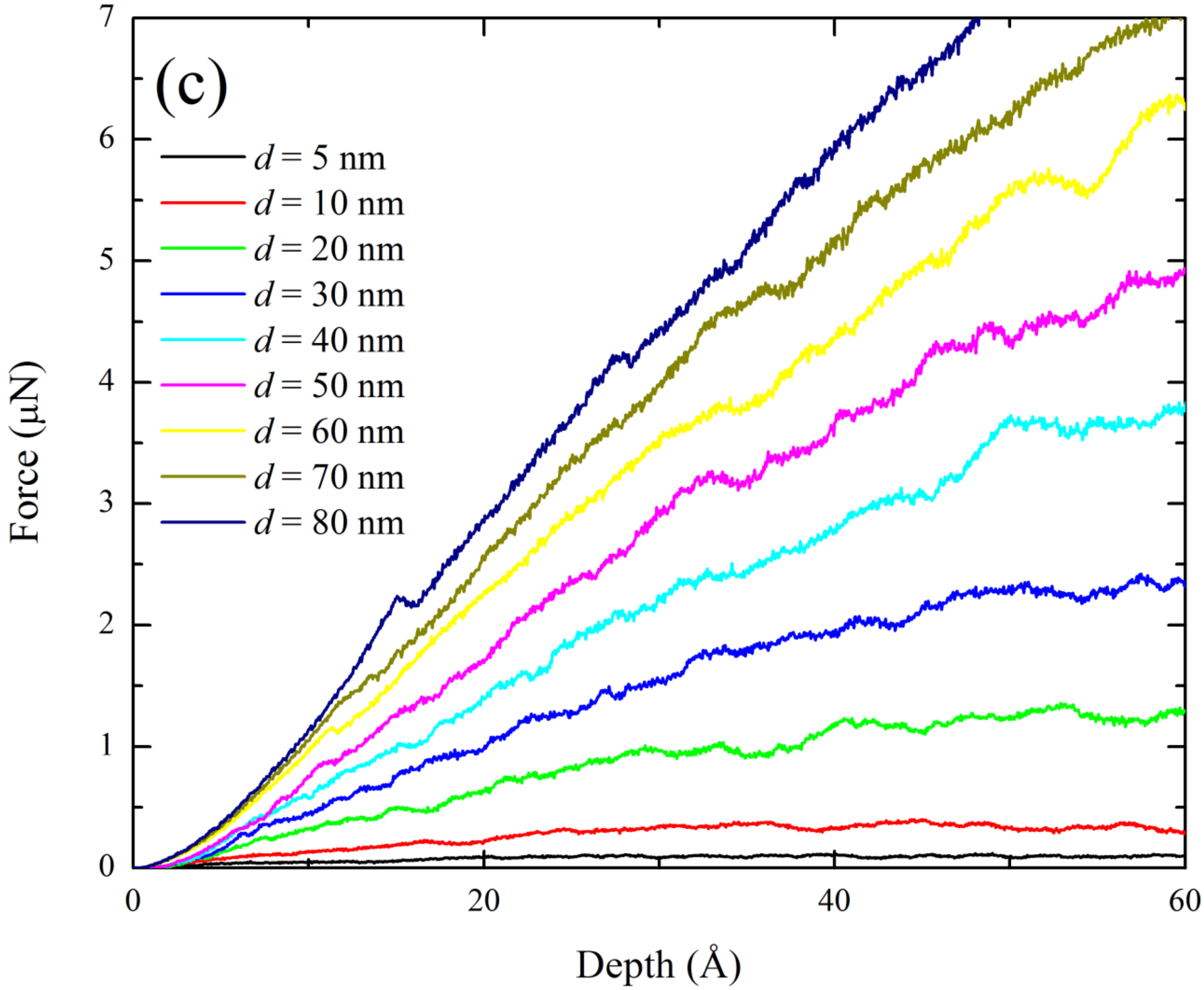

Fig. B1. Effect of the specimen size d on the mechanical response of the Fe specimens under nanoindentation loading. (a) MD-Geo1: loading at (001) surface; (b) MD-Geo2: loading at (110) surface; (c) MD-Geo3: loading at (111) surface.

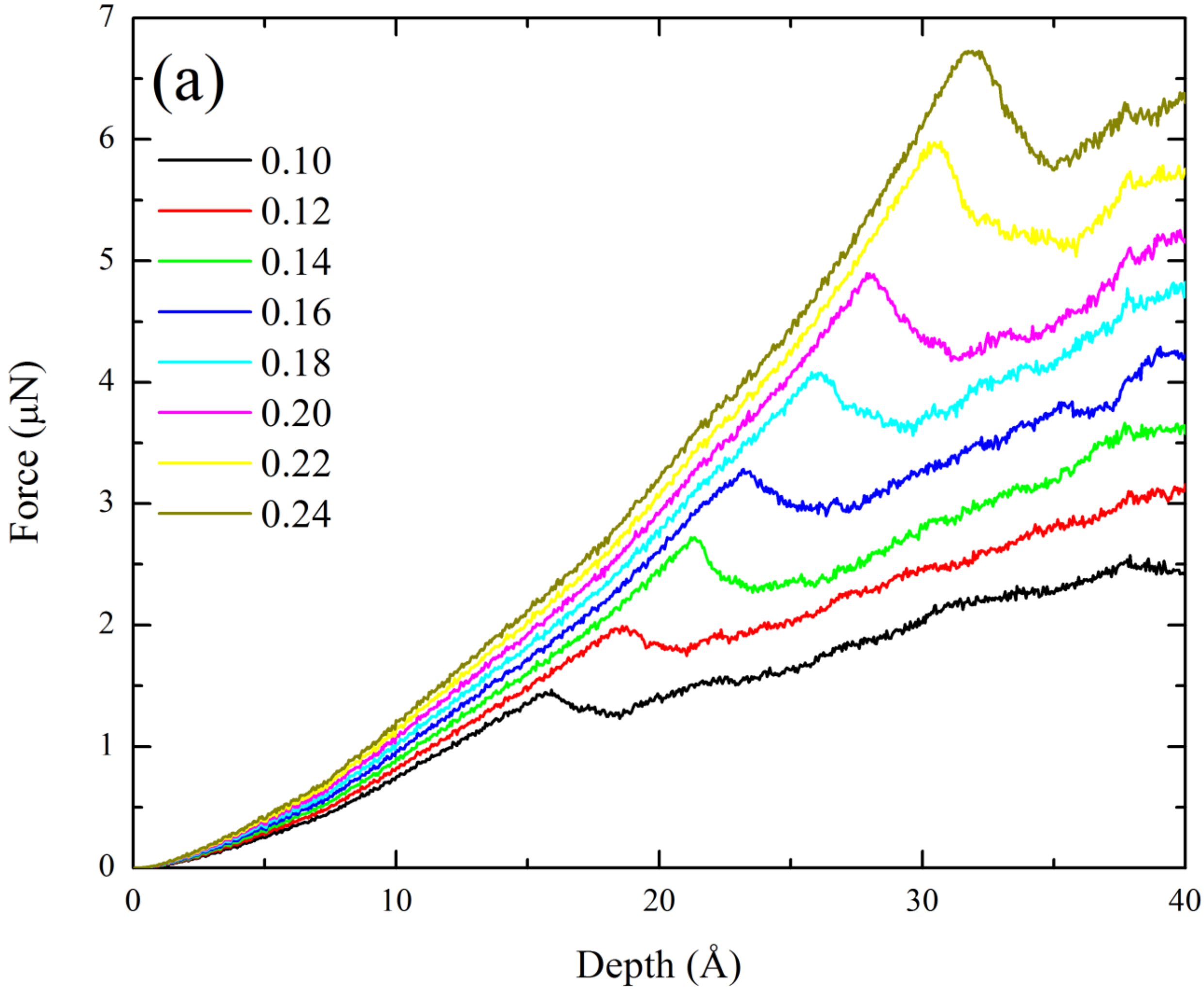
(a)
0.10
0.12
0.14
0.16
0.18
0.20
0.22
0.24
Force (μN)
Depth (Å)
0
1
2
3
4
5
6
7
0
10
20
30
40

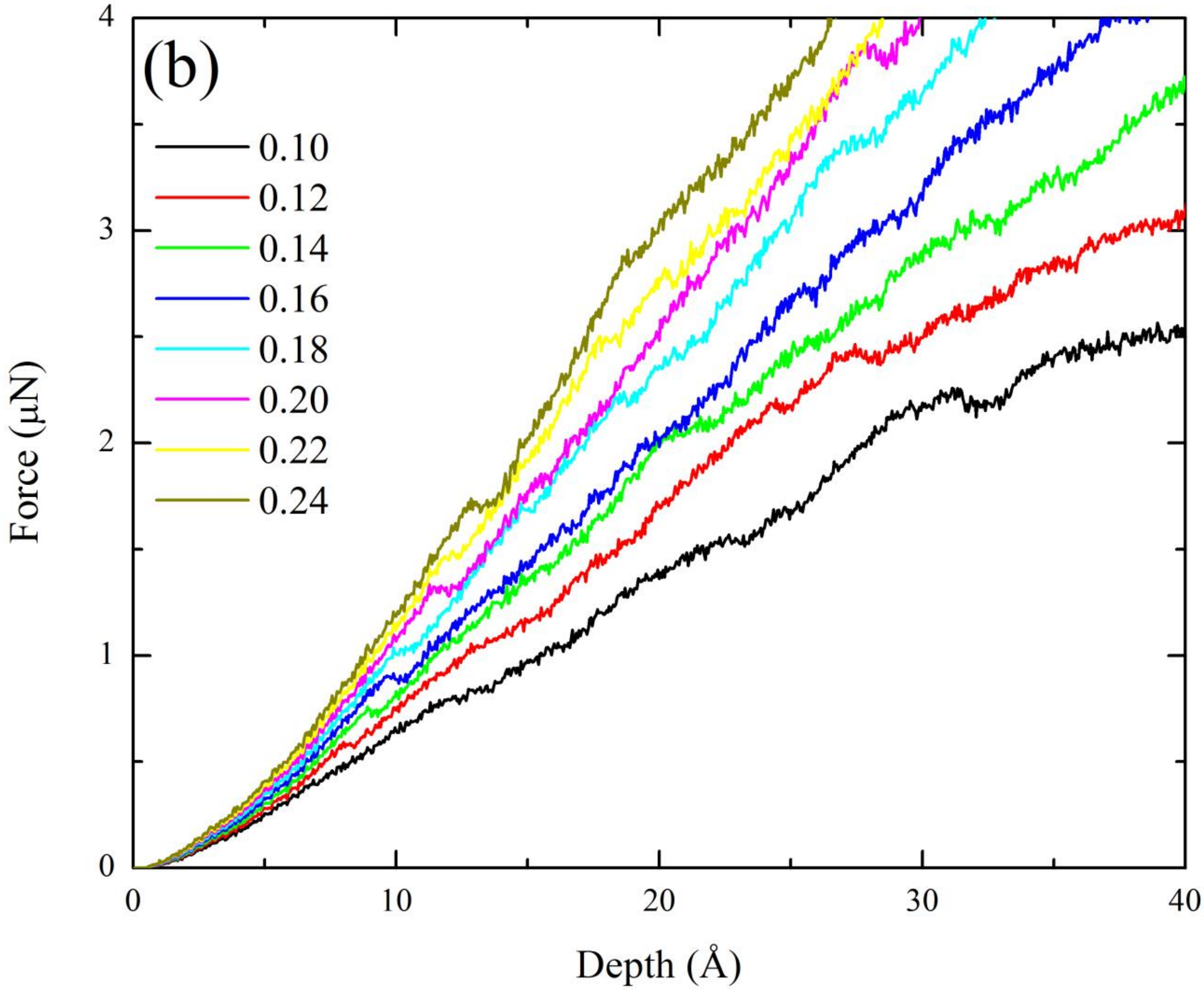
(b)
0.10
0.12
0.14
0.16
0.18
0.20
0.22
0.24
Force (μN)
Depth (Å)
0
1
2
3
4
0
10
20
30
40

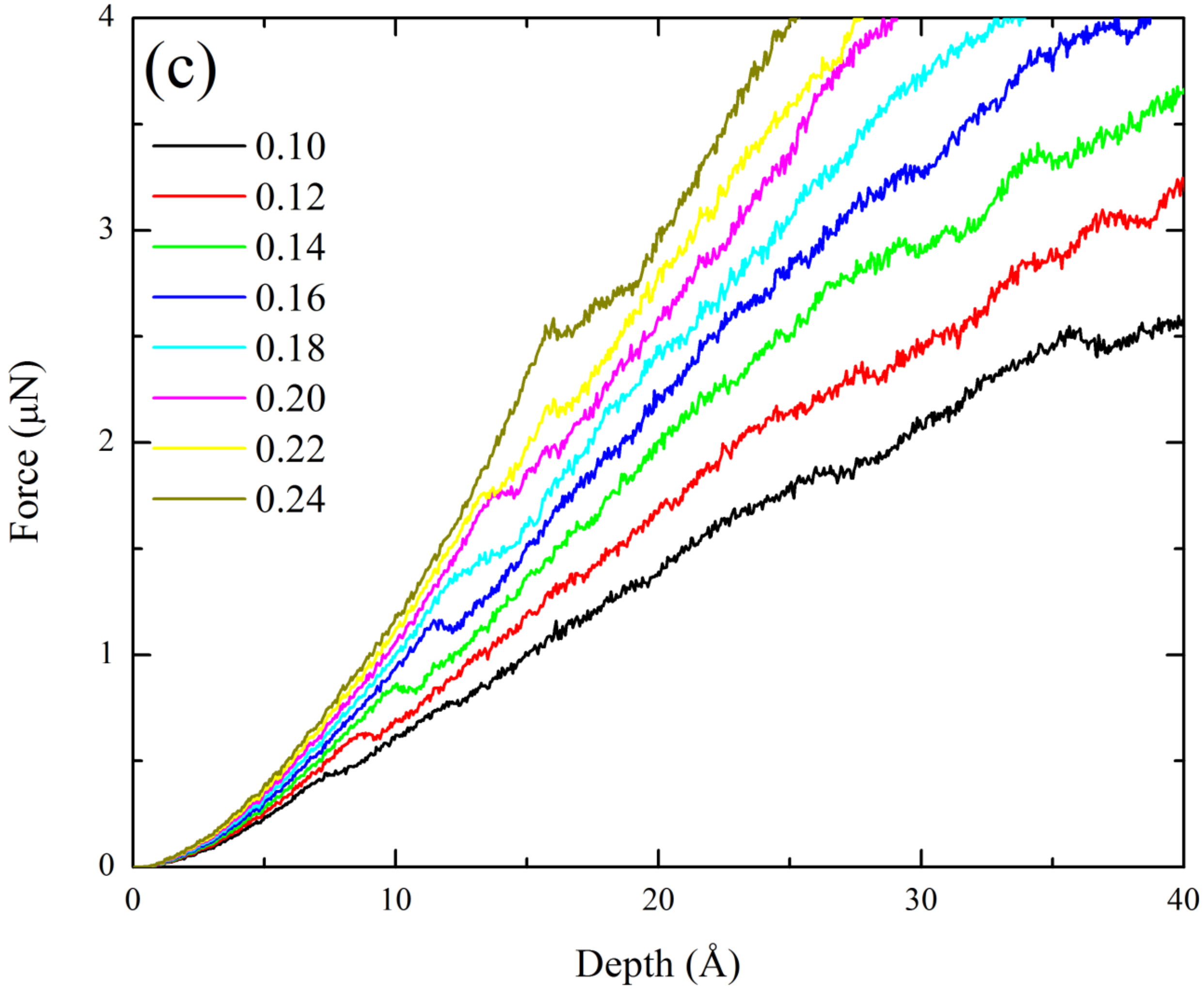

Fig. B2. Effect of the normalized indenter radius R/d on the mechanical response of the Fe specimens under nanoindentation loading. (a) MD-Geo1: loading at (001) surface; (b) MD-Geo2: loading at (110) surface; (c) MD-Geo3: loading at (111) surface.

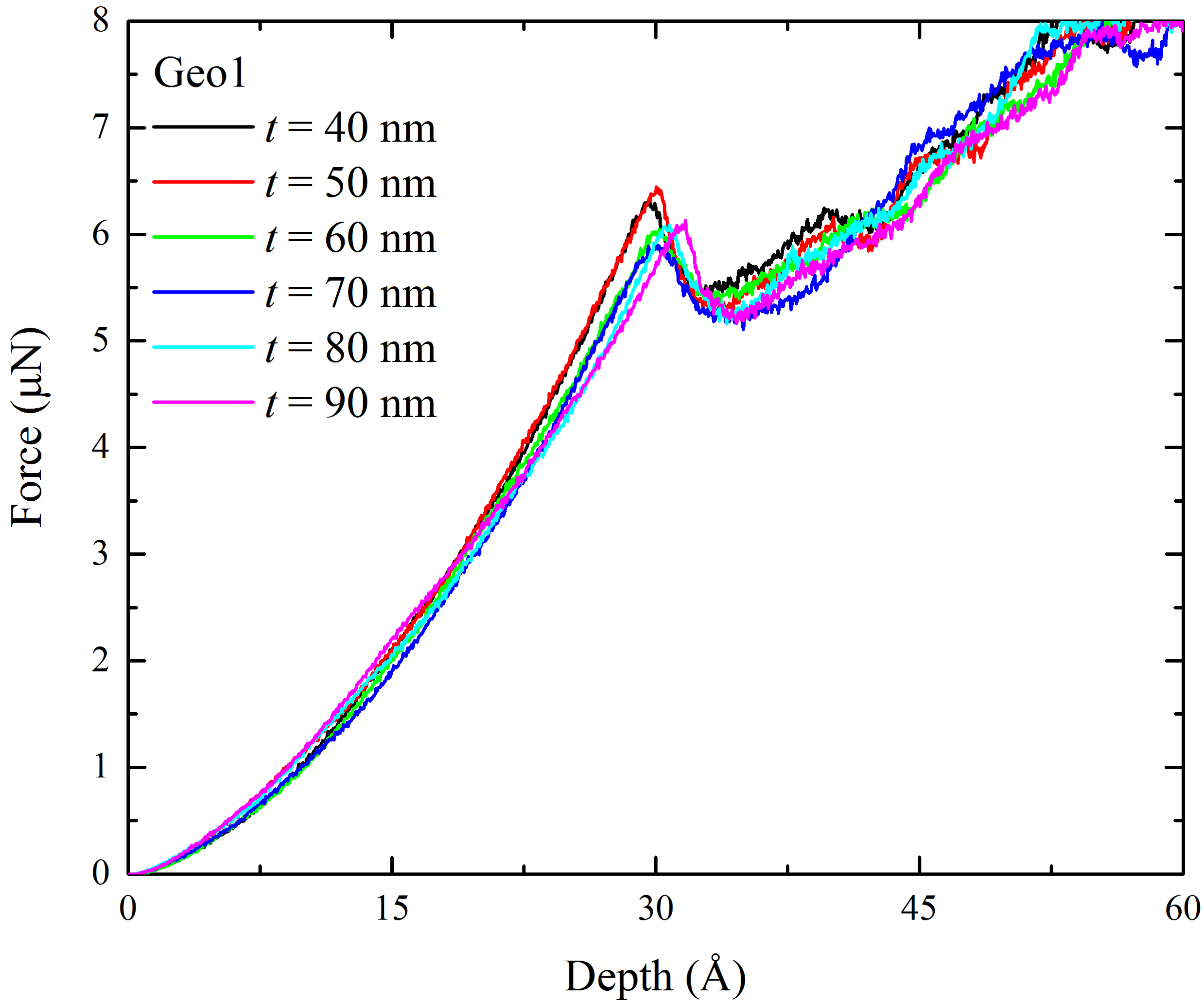
Geo1
t = 40 nm
t = 50 nm
t = 60 nm
t = 70 nm
t = 80 nm
t = 90 nm
Force (μN)
Depth (Å)
0
1
2
3
4
5
6
7
8
0
15
30
45
60

1

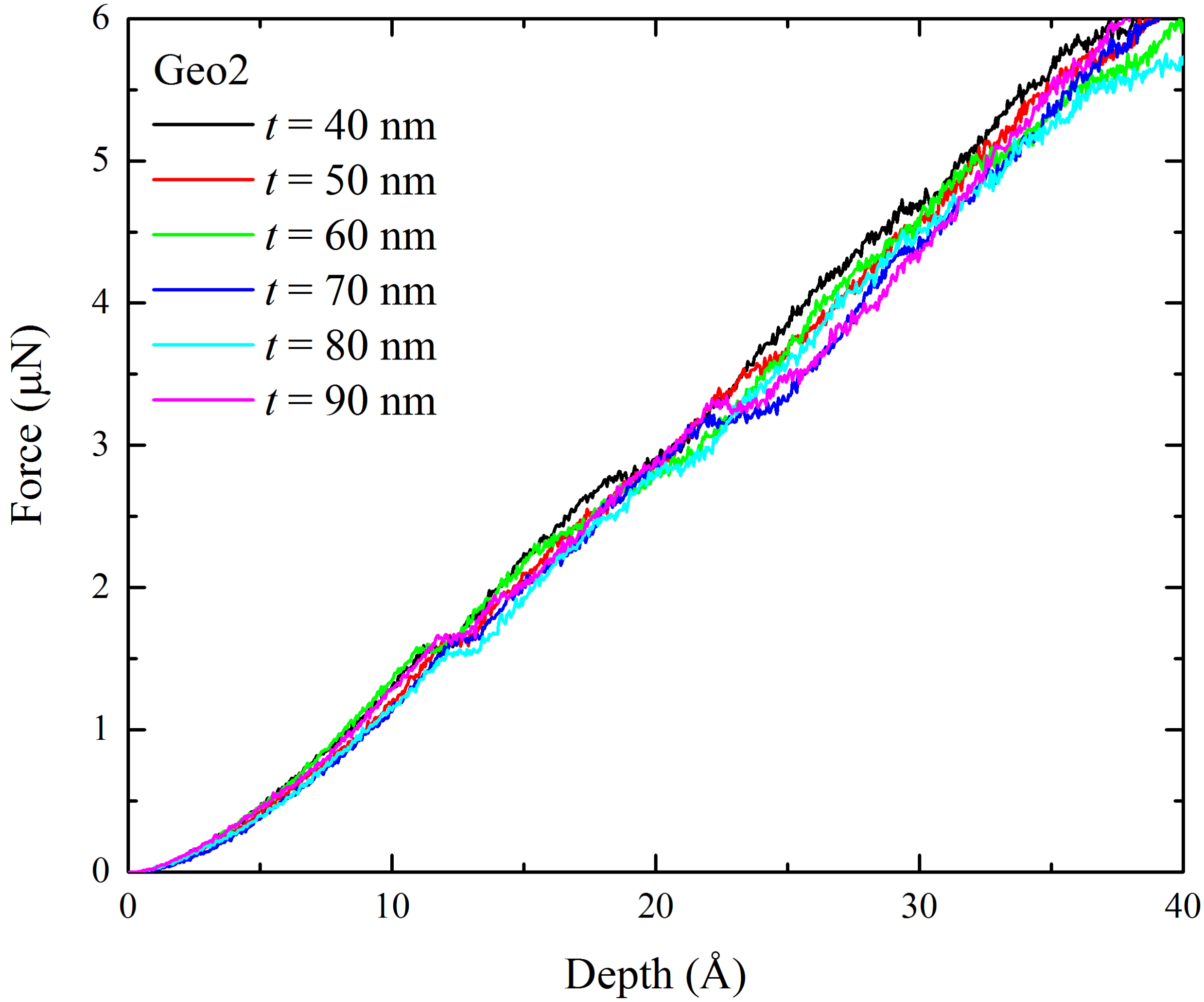

Geo2
t = 40 nm
t = 50 nm
t = 60 nm
t = 70 nm
t = 80 nm
t = 90 nm
Force (μN)
Depth (Å)
0
1
2
3
4
5
6
0
10
20
30
40

1

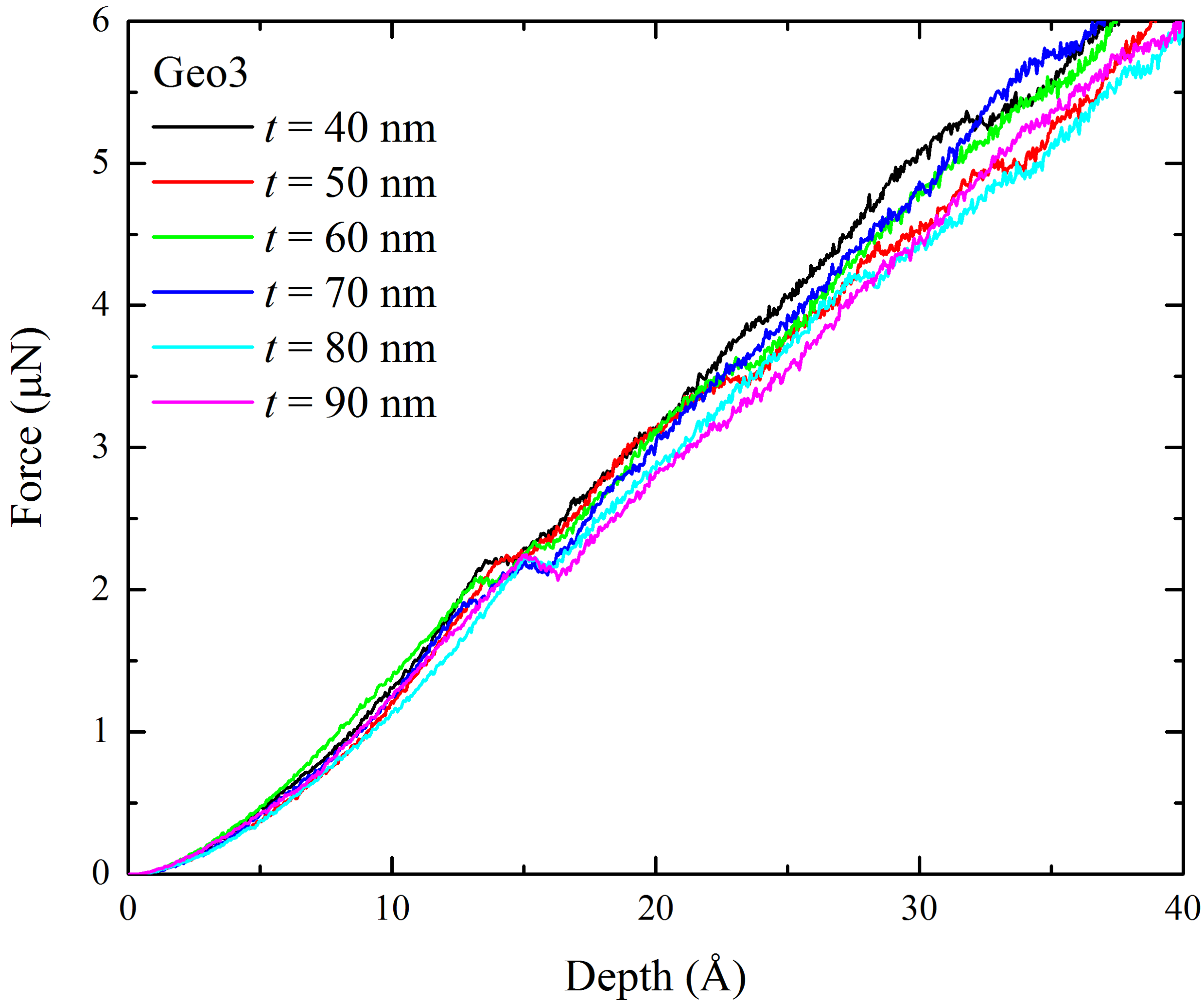

Fig. B3. Effect of the specimen thickness t on the mechanical response of the Fe specimens under nanoindentation loading. (a) MD-Geo1: loading at (001) surface; (b) MD-Geo2: loading at (110) surface; (c) MD-Geo3: loading at (111) surface.